Progress Toward Development of a Multichannel Vestibular Prosthesis for Treatment of Bilateral Vestibular Deficiency

GENE Y. FRIDMAN,* AND CHARLES C. DELLA SANTINA
Department of Otolaryngology—Head & Neck surgery, Johns Hopkins School of Medicine, Baltimore, Maryland

ABSTRACT

This article reviews vestibular pathology and the requirements and progress made in the design and construction of a vestibular prosthesis. Bilateral loss of vestibular sensation is disabling. When vestibular hair cells are injured by ototoxic medications or other insults to the labyrinth, the resulting loss of sensory input disrupts vestibulo-ocular reflexes (VORs) and vestibulo-spinal reflexes that normally stabilize the eyes and body. Affected individuals suffer poor vision during head movement, postural instability, chronic disequilibrium, and cognitive distraction. Although most individuals with residual sensation compensate for their loss over time, others fail to do so and have no adequate treatment options. A vestibular prosthesis analogous to cochlear implants but designed to modulate vestibular nerve activity during head movement should improve quality of life for these chronically dizzy individuals. We describe the impact of bilateral loss of vestibular sensation, animal studies supporting feasibility of prosthetic vestibular stimulation, the current status of multichannel vestibular sensory replacement prosthesis development, and challenges to successfully realizing this approach in clinical practice. In bilaterally vestibular-deficient rodents and rhesus monkeys, the Johns Hopkins multichannel vestibular prosthesis (MVP) partially restores the three-dimensional (3D) VOR for head rotations about any axis. Attempts at prosthetic vestibular stimulation of humans have not yet included the 3D eye movement assays necessary to accurately evaluate VOR alignment, but these initial forays have revealed responses that are otherwise comparable to observations in animals. Current efforts now focus on refining electrode design and surgical technique to enhance stimulus selectivity and preserve cochlear function, optimizing stimulus protocols to improve dynamic range and reduce excitation–inhibition asymmetry, and adapting laboratory MVP prototypes into devices appropriate for use in clinical trials. Anat Rec, 00:000–000, 2012.

Key words: vestibular; prosthesis; implant; areflexia; labyrinth; hypofunction; dizziness; oscillopsia

Abbreviations used: A = anterior; ABR = Auditory Brainstem Response; BVD = bilateral vestibular deficient/deficiency; DPOAE = distortion product otoacoustic emissions; H = horizontal; L = left; LARP = left-anterior/right-posterior; MEMS = microelectromechanical system; MVP = Multichannel Vestibular Prosthesis; P = posterior; R = right; RALP = right-anterior/left-posterior; SCC = semicircular canal; 3D = three dimensional; VLSI = very large scale integration; VOG= video-oculography; VOR = vestibulo-ocular reflex; Z = axis of rotation perpendicular to the horizontal SCC plane; MVP = multichannel vestibular prosthesis.

Grant sponsor: NIH/NIDCD; Grant number: R01DC9255.

*Correspondence to: Gene Y. Fridman, PhD, Vestibular NeuroEngineering Lab, Department of Otolaryngology—Head & Neck surgery, Johns Hopkins School of Medicine, 720 Rutland Avenue, Ross 833, Baltimore, MD 21205. Fax: 410-614-2439. E-mail: gfridma1@jhmi.edu

Received 24 July 2012; Accepted 24 July 2012.

DOI 10.1002/ar.22581

Published online in Wiley Online Library (wileyonlinelibrary.com).

INTRODUCTION

A multichannel vestibular prosthesis (MVP) that senses three-dimensional (3D) head motion using inertial sensors and conveys angular velocity information to the corresponding branches of the vestibular nerve to restore a normal 3D vestibulo-ocular reflex (VOR) could significantly improve quality of life for individuals disabled by bilateral loss of vestibular hair cell function (i.e., bilateral vestibular deficiency [BVD]). In this review, we describe the current status of efforts to develop this technology, surveying relevant preclinical literature, defining technical challenges, briefly discussing preliminary studies with electrical stimulation in human subjects, and summarizing the current status and direction of efforts to realize an MVP for treatment of BVD individuals.

Normal Vestibular Function

Sensation of head rotation, orientation, and translation normally originates in the semicircular canals (SCCs) and otoconial end organs in each labyrinth and is conveyed to the brainstem via five branches of the vestibular nerve. The three SCCs in each ear sense three mutually orthogonal components of 3D head rotation. Fluid in each SCC serves as an inertial load for detecting head rotation about that SCC's axis. Relative motion between the head and the fluid in the SCC causes deflection of the cupula, a gelatinous structure that occludes the canal lumen within a dilated part of the SCC called the ampulla. Deformation of the cupula in turn deflects stereocilia on hair cells in the crista, a sensory neuroepithelium beneath the cupula. These hair cells synapse with primary afferent vestibular neurons and modulate the afferents' firing rates approximately in phase with head angular velocity. Head rotation moving the nose toward the side of a given SCC increases the firing rate of that SCC's afferent fibers above their spontaneous activity, and head rotation in the opposite direction decreases their firing rate. All of the afferent neurons projecting from a given SCC (i.e., in a given ampullary nerve branch of the vestibular nerve) encode head rotation about the same axis and with the same polarity (Carey and Della Santina, 2005).

Each of the three SCCs in each labyrinth is approximately coplanar with a corresponding SCC in the opposite ear: The left anterior and right posterior (LARP) canals, right posterior and left anterior (RALP) canals, and horizontal canals, therefore, define a 3D coordinate system in which the axis of head rotation is encoded by relative activity on each ampullary nerve (Della Santina et al., 2005). The canals are also roughly aligned with the extraocular muscles, an arrangement that minimizes the neural computation needed to generate an accurately aligned 3D VOR. The VOR is mediated by a very fast ($\sim$5–7 ms latency) three-neuron arc (Grossman et al., 1988; Grossman et al., 1989; Tabak et al., 1997a,b; Collewijn and Smeets, 2000; Della Santina et al., 2002; Sadeghi et al., 2006) that maintains stable gaze for head rotations about any axis with velocities as high as 400°/sec and (sinusoidal) frequencies from $\sim$0.05 to $\sim$20 Hz (Grossman et al., 1988; Grossman et al., 1989; Tabak et al., 1997a,b; Collewijn and Smeets, 2000). During head rotations at frequencies below $\sim$0.05 Hz, VOR performance drops with decreasing stimulus frequency. In that region, other oculomotor systems (e.g., smooth pursuit and optokinetic responses) assume a dominant role in maintaining stable gaze (Carey and Della Santina, 2005).

Bilateral Vestibular Deficiency

Chronic profound bilateral loss of vestibular sensation (also called BVD, vestibular areflexia, or vestibular failure) can be caused by ototoxic drug exposure, infection, trauma, ischemia, or other insults to the inner ear (Minor, 1988; Grunbauer et al., 1998; Gillespie and Minor, 1999). Individuals with moderate to severe loss often learn to compensate through participation in vestibular rehabilitation exercise regimens that promote recruitment of multisensory mechanisms for maintaining stable gaze and posture (Herdman, 1998; Herdman et al., 2000). However, there is a limit to the extent other neural systems can replace missing vestibular sensation. Although other oculomotor systems can partially supplant a deficient VOR, the relatively long latency required for visual processing ($\sim$75 ms) causes these systems to fail in stabilizing gaze during quick, high-acceleration head movements for which the VOR normally dominates gaze stabilization (Leigh and Zee, 1999). Predictive mechanisms, motor efference, and the cervico-ocular reflex can also contribute to gaze stabilization when labyrinthine input is deficient (Yakushin et al., 2009; Sadeghi et al., 2010); however, these systems also fail during many passive, high-frequency, high-acceleration whole-body movements encountered during daily activities such as walking and driving. BVD individuals who fail to compensate for their loss through rehabilitation exercises therefore suffer oscillopsia (illusory movement of the visual world during head movements), chronic disequilibrium, and poor postural control.

The prevalence and incidence of chronic profound BVD are difficult to estimate accurately, in part because a lack of standardized diagnostic criteria and effective treatment options precludes use of diagnostic and treatment databases to estimate disease impact. However, data from a health inventory performed on 21,782 adults reveal that approximately 0.1% of US adults report a constellation of symptoms consistent with severe or profound BVD, including visual blurring only during head motion, symptoms lasting more than 1 year, and symptoms rated as at least "a big problem" (National Center for Health Statistics, 2008). Of respondents meeting this BVD case definition, 30% stopped driving because of their problem, 40% missed work (averaging 45 days/year), 60% avoided social activities, and 84% reported a fall in the last 5 years, corresponding an age-adjusted 6.4-fold increase in fall risk compared to other dizzy patients and a 24-fold increase in fall risk compared to the nationwide average (National Center for Health Statistics, 2008; Della Santina and Hoffman, 2010).

Preclinical Studies Supporting Feasibility of a MVP

Evidence that selective stimulation of a SCC can evoke reflexive movements about the axis of that SCC dates back at least to the late nineteenth century, when

Ewald described reflexive head movements in birds during mechanical stimulation of individual SCCs (Ewald, 1892). Tullio and others further characterized these direction-specific reflexes in multiple species (Tullio, 1929; Lowenstein and Sand, 1940). During the 1960s, Suzuki, Cohen, and colleagues conducted an extensive series of experiments using electrical stimulation of vestibular nerve branches (Cohen and Suzuki, 1963; Cohen et al., 1964; Suzuki and Cohen, 1964; Suzuki et al., 1969). They elicited VOR eye responses by delivering monophasic constant-voltage pulses at various pulse rates via 40 μm diameter stainless steel wires inserted near branches of the vestibular nerves in cats, monkeys, and other species. Electrical excitation of a single SCC's ampullary nerve evoked binocular, conjugate VOR eye movements about an axis parallel to the axis of the stimulated SCC, and simultaneous electrical excitation of multiple vestibular nerve branches resulted in 3D VOR responses that were nicely fit by a vector summation of responses to excitation of individual SCCs. Results of these experiments demonstrated that selective electrical pulsatile stimulation of individual vestibular nerve branches can at least partially substitute for normal labyrinthine transduction of head motion. However, capitalizing on these results to make an implantable vestibular prosthesis required technology that was not available in the 1960s, including miniature sensors of head motion, low-power microcontrollers, biocompatible materials, and stimulation paradigms that can safely modulate nerve activity over long durations.

Fortunately, the development of cochlear implants from the 1960s to the present drove creation of much of the technology required to implement a vestibular prosthesis. In particular, cochlear implant development led to clear definition of the biocompatible materials, transcutaneous power transmission technology, and safe electrical stimulation paradigms able to elicit action potentials on peripheral nerves without driving undesirable electrochemical reactions that liberate toxic products at the interface between implanted metal electrodes and biologic fluids. Very large scale integration technology matured in the 1980s and 1990s to yield miniature but computationally powerful microcontrollers. Miniaturization of inertial sensor technology benefitted from an explosion of microelectromechanical systems (MEMS) development in the 1990s and 2000s, largely driven by demand for consumer products such as smart phones and motion-sensing video game controllers.

Although electrical stimulation paradigms like those used by Suzuki and Cohen have been applied countless times in acute neural stimulation studies, monophasic constant-voltage pulses like the stimuli they used were later found to injure tissue when applied over long periods (Shepherd, 1986; Shepherd et al., 1991; Shepherd and Javel, 1999; Merrill et al., 2005). Nearly all chronically implanted neural stimulation systems now in use deliver brief (typically <1 ms/phase) biphasic, charge-balanced current pulses rather than monophasic or constant voltage pulses. Furthermore, these pulses are delivered using relatively large (>0.1 mm^2) surface PtIr electrodes rather than small diameter stainless steel wires, to ensure current densities that remain within a range defined by "safe charge-injection criteria" (Rose and Robblee, 1990; Shannon, 1992; Merrill et al., 2005; Wilson and Dorman, 2008).

Drawing on Suzuki and Cohen's findings and incorporating new technologies that allowed design of a miniature, chronically head-mounted stimulator, Gong and Merfeld demonstrated the first self-contained vestibular prosthesis for preclinical use in animal studies (Gong and Merfeld, 2000; Gong and Merfeld, 2002). Small enough to be affixed to the head of a guinea pig, this device used a single-axis MEMS gyroscope to sense head rotation about the mean horizontal SCC axis, and it delivered constant-current, charge-balanced, biphasic pulses to an electrode implanted in one SCC (typically a horizontal SCC) of a guinea pig rendered BVD via surgical plugging of otherwise normal SCCs. Modulation of pulse frequency elicited $\sim 10^\circ$/sec peak VOR eye response during sinusoidal prosthesis rotation, and step changes in pulse rate evoked transient responses up to 100°/sec peak eye velocity. Response velocity increased both with increasing pulse rate and with increasing pulse amplitude.

Extending this approach to 3D, the Johns Hopkins Vestibular NeuroEngineering Lab's *MVP1* (Fig. 1A) incorporated three mutually orthogonal gyroscopes that sense 3D head rotational velocity, eight electrodes, and a single current source shared between electrode pairs activated in pulse-frequency-modulated fashion (Della Santina et al., 2007). Each component of head angular velocity mapped to changes in pulse frequency on an electrode in the corresponding SCC (Fig. 1B), using a nonlinear function designed to emulate the normal dependence of vestibular afferent firing rates on head angular velocity (Fig. 1C). When tested in chinchillas rendered BVD through intratympanic injections of the ototoxic aminoglycoside antibiotic gentamicin, this device partially restored VOR responses appropriate to stabilize gaze significantly during head rotation about any SCC axis (Fig. 1D).

Although these experiments provided encouraging results supporting the feasibility of an MVP for clinical use, they also identified key challenges, particularly during attempts to encode high-velocity, high-acceleration head movements (for which prosthetic stimuli must be relatively intense). First, electrical current intended for a given branch of the vestibular nerve spreads to excite not only its target branch but also neighboring branches, resulting in misalignment of VOR responses. Second, VOR asymmetry was evident, with eye movement responses to upmodulation of pulse rate (corresponding to head rotation toward the implanted side) stronger than responses to downmodulation (corresponding to inhibitory head rotations). Although excitation–inhibition asymmetry is a property of many elements within the neural circuitry mediating the normal VOR (for example, changes in hair cell neurotransmitter release can drive vestibular afferent firing rates up to $>4\times$ baseline firing rate but can only inhibit firing rates to zero), the problem can be especially acute for prosthetic stimulation, because unlike normal hair cells, an MVP cannot downmodulate a vestibular afferent's firing rate below that afferent's spontaneous rate. These two constraints on MVP performance—misalignment owing to current spread and excitation–inhibition asymmetry compromising the ability to encode inhibitory head rotations—are key challenges to realization of an effective MVP for clinical use. Recent efforts to overcome these challenges are discussed below.

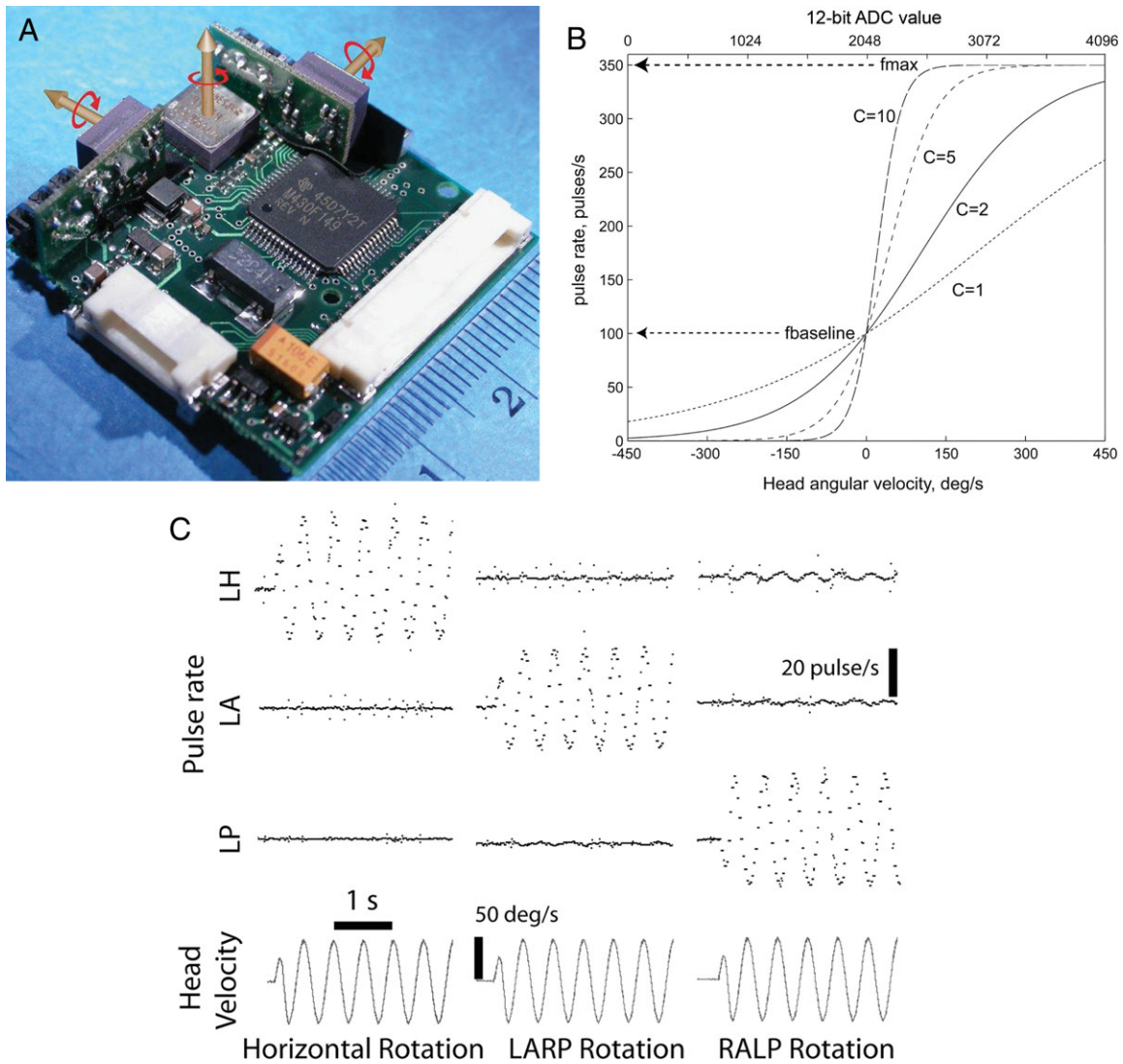

Fig. 1. Johns Hopkins MVP1 multichannel vestibular prosthesis. (A) MVP1 is designed for conducting acute and chronic vestibular stimulation animal experiments. A top view of the 31 × 31 × 11 mm^3 device shows the three orthogonally oriented gyroscopes and the microcontroller. (B) Functions used by MVP1 to map head angular velocity to pulse rate delivered to the corresponding electrode channel. (C) Bench tests of the prosthesis show output of the device directed to three electrode channels as the prosthesis is rotated sinusoidally about each of the three gyroscope axes (Horizontal, LARP, and RALP). (D) Experimental results obtained from chinchillas implanted with intralabyrinthine electrodes show partial restoration of 3D VOR eye responses to head rotations about Horizontal, LARP, and RALP axes. Reprinted with permission from Della Santina et al., IEEE Trans Biomed Eng, 2007, 54:1016–1030.

Specific circuit elements differ between different vestibular prosthesis prototypes, but most share a common basic design scheme (Fig. 2) (Gong and Merfeld, 2000; Gong and Merfeld, 2002; Della Santina et al., 2007; Chiang et al., 2011). Head rotation is sensed using motion sensors, which are typically either single-axis sensors (Gong and Merfeld, 2000; Gong and Merfeld, 2002) or three-axis MEMS gyroscopes (Della Santina et al., 2007; Chiang et al., 2011). Gyroscope signals are filtered digitally and/or via analog circuitry to attenuate noise and frequency components outside the range of normal SCC performance. Additional filtering may be performed in an attempt to better fit the dynamics and latency of electrically evoked responses to natural VOR responses.

In most prostheses described so far, a microcontroller modulates the pulse *frequency* of biphasic current pulses to encode the sampled rotational velocity signal (Gong and Merfeld, 2000; Gong and Merfeld, 2002; Della Santina et al., 2007; Chiang et al., 2011). In a MVP such as the Johns Hopkins MVP1 (Della Santina et al., 2007) and MVP2 (Chiang et al., 2011), the filtered signals from each of three mutually orthogonal gyros are sampled and assembled into a vector representing 3D head angular velocity. Rather than simply passing each gyro's signal directly to the circuit or software module that modulates pulse frequency on the single SCC best aligned with that gyro, the microcontroller performs a directional correction, multiplying the 3D data vector by a fitting matrix M (further discussed below) to correct

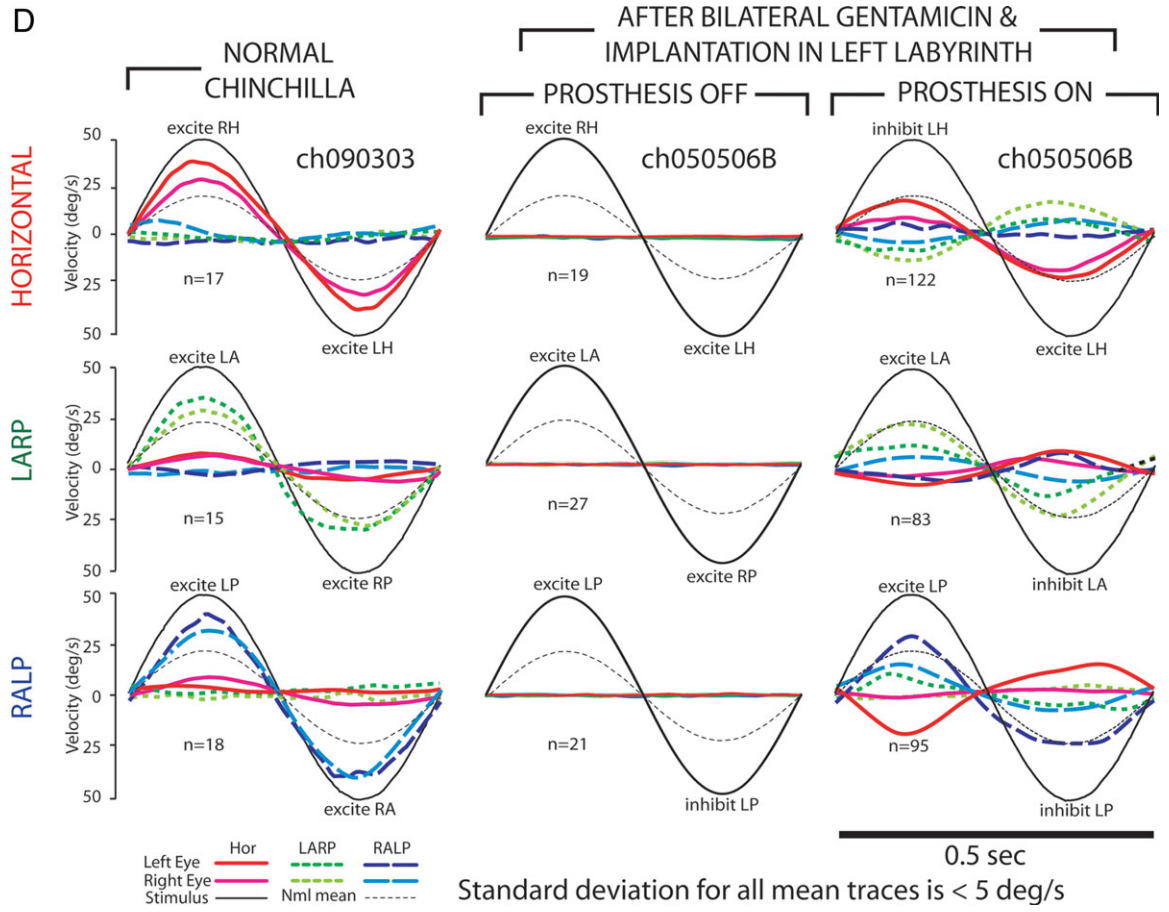

Fig. 1. (Continued)

for misalignment between the actual axis of head movement and axis of VOR eye responses that would otherwise occur when current intended for one SCC's ampullary nerve spreads to other vestibular nerve branches (Fridman et al., 2010). In addition to directional correction, signals are mapped from sensed rotational speed (in °/sec) to stimulation pulse rate and/or amplitude, typically using a sigmoidal relationship like the ones shown in Fig. 1B.

As with all commercially available cochlear implants, MVP stimulation pulses are typically biphasic and charge-balanced between phases (Bonham and Litvak, 2008). This prevents electrode corrosion and evolution of gas or other toxic substances that would otherwise occur at each electrode's metal–saline interface owing to Faradaic (oxidation–reduction) reactions (Rose and Robblee, 1990; Merrill et al., 2005). The first phase is typically cathodic, because cathodic current is typically the excitatory phase for neural tissue near an extracellular electrode. The anodic phase is only included to maintain charge balance over a millisecond time scale. Some MVP stimulus paradigm implementations also allow pulses to be asymmetric, typically using a "cathodic pseudomonophasic" approach in which a relatively brief and high-amplitude cathodic phase is charge-balanced by a relatively long and low-current anodic phase (Hayden et al., 2011; Macherey et al., 2011).

The MVP2 contains multiple, independent current sources that allow the microcontroller to distribute stimulus current across multiple electrodes simultaneously in tripolar and quadropolar arrangements intended to steer current toward target axons and away from nontarget tissue (Chiang et al., 2011). Similar current steering approaches have yielded improved spatial resolution in cochlear implants (Bonham and Litvak, 2008).

KEY CHALLENGES AND EFFORTS TO OVERCOME THEM

Although preclinical studies have provided ample data to suggest that a MVP will be effective in clinical application, they have also identified several challenges that must be overcome to ensure optimal performance. Current research largely centers on addressing these challenges.

Current Spread and VOR Misalignment

Initial tests of the MVP conducted on chinchillas and rhesus monkeys rendered bilaterally vestibular deficient via treatment with intratympanic gentamicin demonstrated partial restoration of the normal 3D VOR; however, misalignment between the expected and the actual axis of eye rotation responses was apparent in

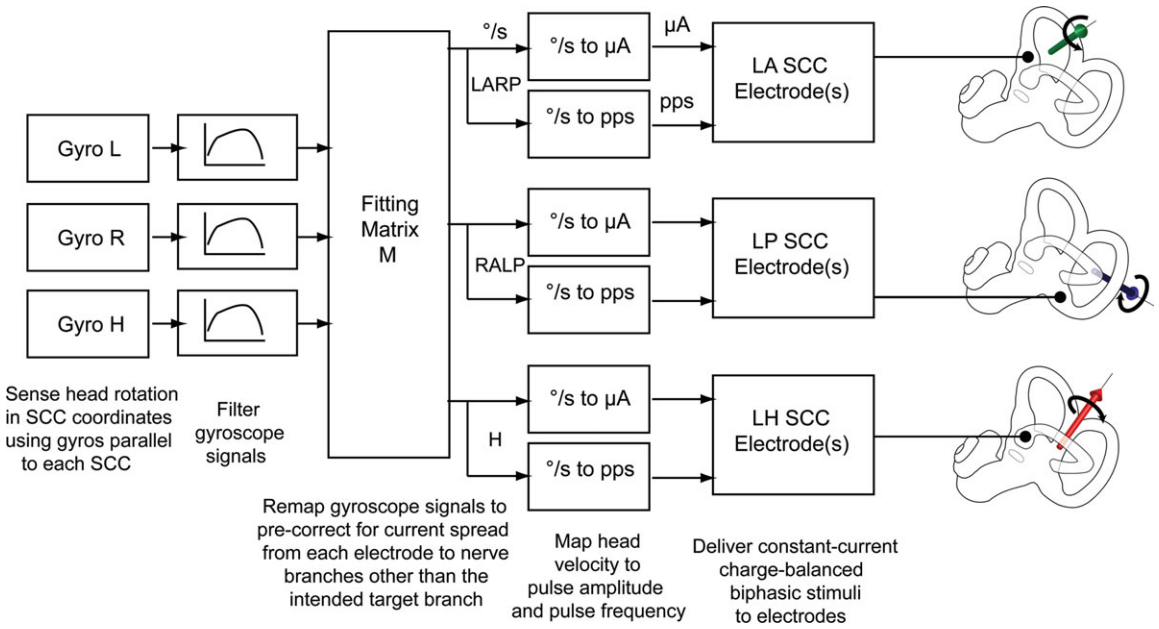

Fig. 2. Common signal processing elements used in vestibular prosthesis design. Gyroscopes sense head rotation about each axis corresponding to the SCC orientations. These angular velocity signals are filtered to more closely emulate the transfer function of the SCC hydrodynamics. Linear coordinate transformation uses matrix *M* to precorrect for misalignment between the axis and the velocity of the actual head rotation, and those of the head movement sensation evoked by electrode stimulation. The corrected velocity signals are then mapped to amplitude and pulse rate specifications for each electrode implanted in the LARP, RALP, and Horizontal SCCs. These pulse-rate and pulse-amplitude specifications are combined with constant stimulus parameters (stimulation and reference electrode selection and pulse-width of current pulses) by the pulse-generation algorithm and circuitry to deliver biphasic charge-balanced stimuli to the electrodes. The same algorithm schedules the delivery of each pulse and ensures that the pulses delivered to the different electrodes do not overlap in time.

each case (Della Santina et al., 2007; Dai et al., 2011b). For example, Fig. 3 shows that stimuli delivered by an electrode implanted in the left posterior SCC of a chinchilla elicit VOR responses predominantly about the RALP axis at low and moderate stimulus current amplitudes during 2-Hz pulse frequency-modulated stimulation. However, at higher currents, the mean axis of eye movements shifted away from the RALP axis, suggesting spurious activation of nontarget ampullary nerve branches owing to spread of stimulus current beyond the intended target. Moreover, disconjugacy (disparity between the axes of rotation of the left and right eyes) also became apparent, suggesting spurious stimulation of the utricular and/or macular nerve. To the extent that VOR-driven eye movements are an accurate indicator for perception of head motion, increased current spread causes not only decreased visual acuity but also misperception of head movement direction.

Four main approaches have been used to improve stimulation selectivity: (1) optimization of electrode design and surgical placement, (2) stimulation parameter optimization, (3) precorrection of misalignment using linear algebraic techniques, and (4) reliance on directional plasticity of vestibulo-cerebellar neural circuits.

Optimization of Electrode Design and Surgical Placement

Accurately targeting each SCC nerve branch via precise surgical placement of electrodes in the vestibular labyrinth can maximize electrode-nerve coupling with the target ampullary nerve branch while minimizing misalignment owing to spurious stimulation of nontarget branches. Hayden et al. extensively modeled current flow within the implanted chinchilla labyrinth, developing a finite element model based on precise anatomy, coupling that model's potential field predictions with a stochastic neuromorphic model incorporating 2415 model vestibular afferent fibers and realistic temporal dynamics, and then comparing model predictions of population activity in each nerve branch to quantitative measurements of 3D VOR responses (Hayden et al., 2011). This model has recently been extended to the rhesus monkey labyrinth (Hedjoudje et al., 2012). In both cases, model predictions fit empiric data well, suggesting that such models can facilitate electrode design optimization. In both model simulations and empiric experiments, monopolar stimulation via a single active electrode in each ampulla (with current returned via a distant electrode outside the labyrinth) achieves strong coupling with the target nerve branch but also significant current spread to nontarget branches, and hence adequately selective responses can only be achieved when the active monopolar electrode is very close to the target nerve. In contrast, bipolar electrode pairs positioned transverse to the axis of the ampulla and perpendicular to the distal trajectory of the target nerve elicit more focal stimulation and greater selectivity, but they must be positioned precisely to achieve these benefits. These findings led to electrode array designs that incorporate a trio of electrodes within each of three silicone leads designed to self-orient when surgically inserted into the ampullae (Chiang et al., 2011). By positioning multiple electrode contacts near the sensory neuroepithelium of each SCC,

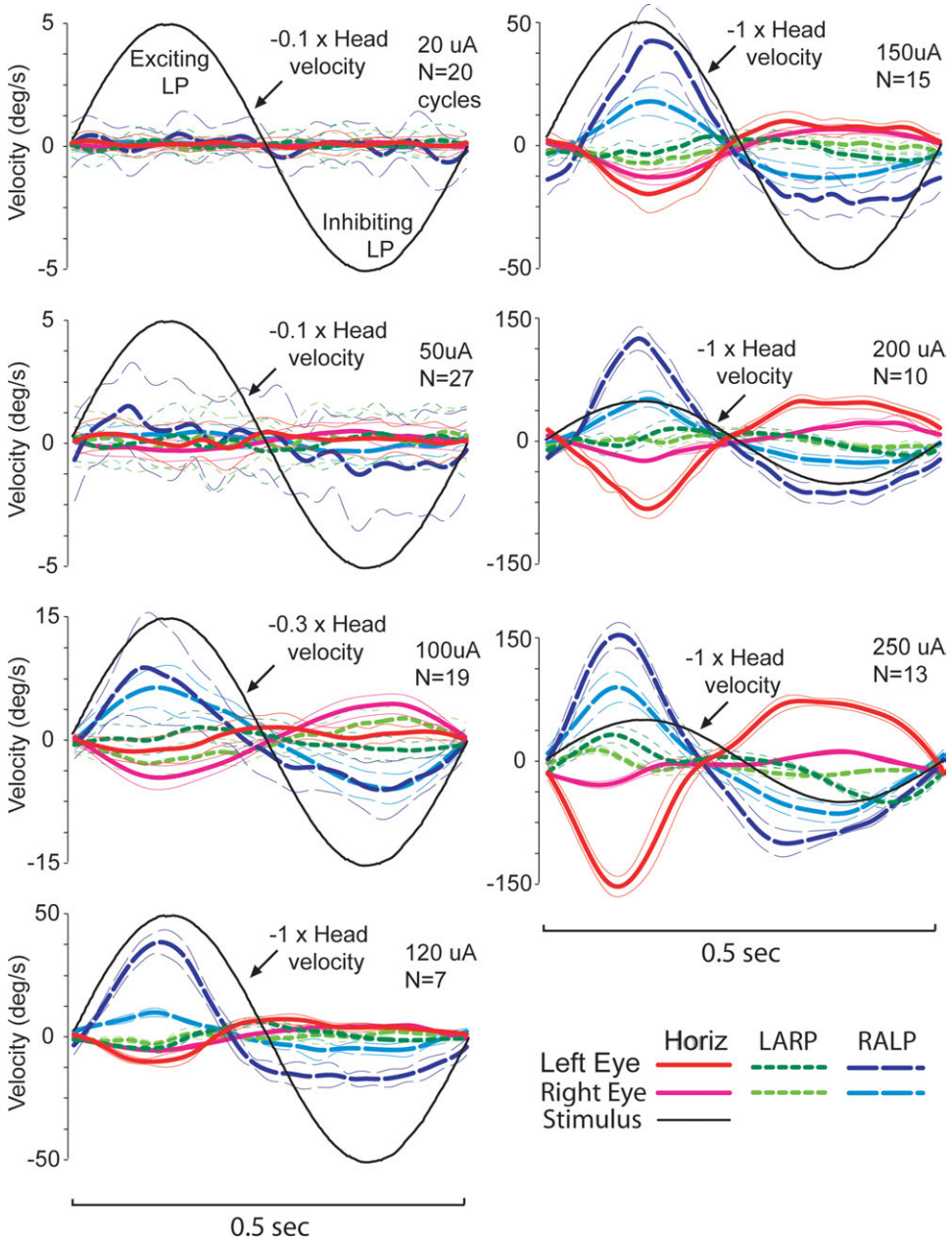

Fig. 3. VOR responses during a 2 Hz, 50°/sec RALP head rotation encoded by prosthetic stimulation delivered by a monopolar electrode in the LP SCC ampulla with respect to a distant reference. For each panel, stimulus current is labeled; all other parameters were kept constant. In each, the ordinate axis and inverted head velocity trace have been scaled to enhance visibility all components of the response. Barely visible at 50 μA, the response at 100 μA includes conjugate RALP rotations similar to normal chinchilla responses, except for a horizontal component that could indicate spurious stimulation of the horizontal SCC ampullary nerve or the otolithic endorgans. At 250 μA, the LP response has grown to over 150°/sec peak velocity, but the spurious horizontal component nearly equals it. Reprinted with permission from Della Santina et al., IEEE Trans Biomed Eng, 2007, 54:1016–1030.

these electrode designs increase the probability that least one electrode will be adjacent to the target tissue, allow the use of bipolar and tripolar stimulation paradigms (Chiang et al., 2011), and facilitate estimation of how stimulation coupling and misalignment depend on electrode location.

An additional benefit of having multiple electrode contacts in the vicinity of the target neurons is that while one of the electrode contacts is used for stimulation, another can be used to record electrically-evoked compound action potentials (ECAPs). ECAP waveforms collected with vestibular prosthesis electrodes are similar in amplitude and latency to those obtained from the cochlea using cochlear implants. Unlike VOR responses, ECAPs are not affected by general anesthesia, and hence intraoperative monitoring of ECAP amplitudes during

electrode implantation can be used to facilitate optimal surgical positioning of electrodes (Chiang et al., 2011; Nie et al., 2011). Correlation of VOR magnitude, VOR misalignment, and ECAP magnitudes reveals that a 200-μm change in electrode location within the ampulla is sufficient to cause a large change in performance in rhesus monkeys (Dai et al., 2012a).

Although both modeling and empiric measurements demonstrate that bipolar electrode pairs can achieve more selective stimulation than monopolar electrodes that pass current returned via a distant reference electrode outside the labyrinth, bipolar stimulation requires that the two electrodes be positioned with much greater precision than required for monopolar electrodes. As a compromise between these two extremes, our group recently described the use of a reference electrode implanted in the crus commune of the anterior and posterior SCCs (Fridman et al., 2010; Chiang et al., 2011). Fortuitously, this arrangement steers current from each active electrode toward the corresponding ampullary nerve and away from the facial nerve, improving stimulation coupling with target tissue, reducing misalignment, and reducing the likelihood of spurious facial nerve excitation.

Refinement of Stimulus Parameters

Once optimal electrode positioning has been achieved, optimization of stimulus amplitudes and timing can further improve device performance. A pulse frequency modulation scheme can encode head angular velocity over a wide dynamic range while minimizing changes in the axis of eye movement responses, whereas modulating pulse current amplitude to encode head velocity (which is closer to the standard approach used for encoding spectral band intensities in cochlear implants) can encode head velocity over only a small dynamic range before incurring marked increases in VOR misalignment owing to current spread (Davidovics et al., 2010). When a prosthesis encodes head angular velocity in terms of the depth of pulse frequency modulation using symmetric, biphasic constant-current pulses of a given charge/phase, shorter pulse durations achieve better misalignment for a given response magnitude than do longer pulse durations (Davidovics et al., 2010). This effect is somewhat surprising, because shorter pulse durations require higher current amplitude to evoke a given VOR response velocity, and higher currents typically imply greater current spread and misalignment.

Vector Precompensation—Correction of 3D VOR Misalignment Using Linear Algebraic Techniques

Despite optimization of electrode design, surgical positioning and stimulus timing, some current spread and resulting misalignment will always occur. The consequences of this misalignment can be thought of as a warping of the 3D coordinate system defined by the axes of the SCCs. If current intended to stimulate only the horizontal SCC ampullary nerve spreads to excite the nearby anterior SCC ampullary nerve, then stimuli meant to encode purely horizontal head rotations will inadvertently convey a pattern of vestibular nerve activity that would normally occur during head rotation about an axis partway between the horizontal and the anterior SCC axes.

A linear coordinate transformation can be used to adjust intensity on each of three electrodes to compensate for misalignment owing to current spread (Fridman et al., 2010). This method involves first measuring the 3D axis of VOR responses for each of a large number of head rotation axes and then computing the 3×3 fitting matrix that describes a least-squares-optimal mapping from those actual responses to the ideal/desired VOR response axes that would have occurred had there been no current spread (Fig. 4). The MVP microprocessor subsequently multiplies each three-vector of sampled head angular velocity by this fitting matrix in real time, effectively converting any desired VOR eye movement to the electrode intensity combination needed to evoke that desired movement despite current spread. An additional benefit of this method is that the fitting matrix also corrects for dependence of response magnitude on eye movement direction. Moreover, the remapping can be implemented either with a single matrix M or a family a matrices M_i ($i = 1$–8) optimized for different octants of 3D head rotation space or for different shells of that space (representing different ranges of head rotational speed) (Rahman, 2011). Experiments conducted on chinchillas revealed that this approach yielded a ~50% reduction in misalignment while also achieving more uniform response velocities (Fridman et al., 2010). Subsequent extension of this approach to monkeys resulted in a similar improvement, particularly when a set of fitting matrices specific to each octant of the 3D space of possible head rotation axes was implemented (Davidovics et al., 2012).

Directional Plasticity of Vestibulo-Cerebellar Neural Circuits

Residual VOR misalignment that persists despite optimization of electrode design, surgical technique, stimulus timing, and orthogonalization transformations can still be great enough to compromise visual acuity by making the eyes move about an axis that differs from the axis of head rotation. Fortunately, vestibulo-cerebellar circuits serving the VOR are adept at correcting for directional errors over time. When animals with normal labyrinths are exposed to abnormal visual conditions that lead to a visual-vestibular directional mismatch (e.g., a cat pitched up and down while positioned within a well-lit cylindrical drum than moves horizontally in time with the cat's vertical motion), the VOR adapts over about 30 min to better align reflexive eye movements with apparent motion of the visual field (Schultheis and Robinson, 1981). By analogy to this *cross-axis adaptation* effect in normal animals exposed to abnormal visual conditions, VOR directional plasticity also reduces misalignment significantly over the first week of MVP stimulation in chinchillas and in rhesus monkeys (Dai et al., 2010a; Dai et al., 2011a) (Fig. 5). Lewis et al. observed similar results in monkeys stimulated via an electrode in the posterior SCC but coupled to a motion sensor aligned to best measure horizontal head rotation (Lewis et al., 2001; Lewis et al., 2002).

Although the directional adaptation capacity of vestibulo-cerebellar circuits is impressive, both the duration required to achieve a maximally aligned VOR and the

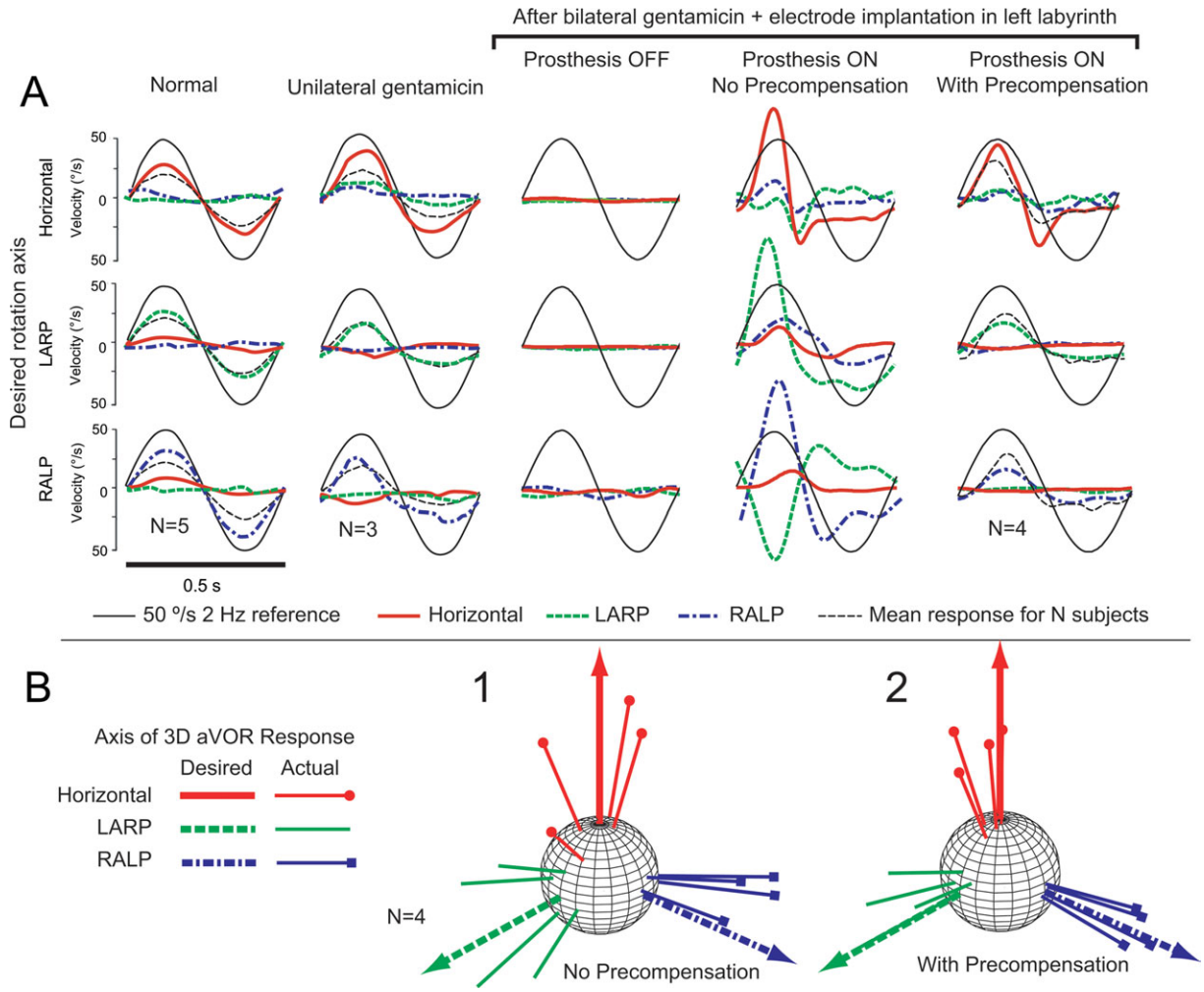

Fig. 4. (A) Precompensatory remapping improves both axis and amplitude of prosthesis-encoded head velocity percepts as measured by 3D VOR responses in chinchillas. **Column 1**: Mean head and eye velocity for a normal chinchilla during 50°/sec peak 2 Hz whole-body rotations in darkness about the axis of each coplanar pair of SCCs: Horizontal (top row), LARP (middle row), and RALP (bottom row). For clarity, only mean responses are shown; the standard deviation for each trace was <6°/sec. Eye traces are inverted to compare with head. Normal chinchillas exhibit good alignment with head rotation axis and symmetric gain (eye velocity/head velocity) of about 0.5. Dashed curves indicate mean responses for all animals studied. **Column 2**: VOR responses for chinchillas treated with intratympanic gentamicin (ITG) in one ear are attenuated during ipsilesional rotation. **Column 3**: Head rotation of a bilaterally vestibular-deficient animal after ITG and canal plugging elicits no response for any axis when prosthesis is off. **Column 4**: Responses for the same animal when pulse rates on individual electrodes implanted in the left labyrinth SCCs are modulated without precompensatory 3D remapping. Misalignment owing to current spread is evident for all three axes of rotation. **Column 5**: VOR responses of the same animal to stimuli with precompensatory 3D remapping are more like those of animals with a single working labyrinth (Column 2). (**B**) 3D VOR responses to prosthetic stimuli encoding head rotation about each of the three SCC axes *without* (B1) and *with* (B2) precompensatory 3D remapping, for each of four implanted chinchillas. Reprinted with permission from Fridman et al., J Assoc Res Otolaryngol, 2010, 11:367–381.

remaining steady-state misalignment when a plateau of performance is reached are both smaller when the initial error that must be corrected is smaller. Therefore, achieving a well-aligned 3D VOR will likely require a combination of programmatic and neural contributions to reducing misalignment.

Excitation-Inhibition Asymmetry

Excitation–inhibition asymmetry is a normal feature of the labyrinth and neural elements underlying the VOR: hair cells, primary vestibular afferents, and secondary vestibular neurons each possess a greater dynamic range for excitation than for inhibition (Carey and Della Santina, 2005). In a normal subject, these asymmetries are masked by the fact that secondary vestibular neurons effectively compute the difference between inputs from SCCs arranged in antiparallel, coplanar pairs. Engineers routinely use an analogous approach to expand the linear dynamic range of strain gauge sensors with asymmetric nonlinear responses. Placing two identical sensors in antiparallel on the device under test and then connecting their outputs to a differential amplifier yields a system with twice the sensitivity of either sensor alone, zero offset, and a linear response over a wider dynamic range (Berger et al., 1996).

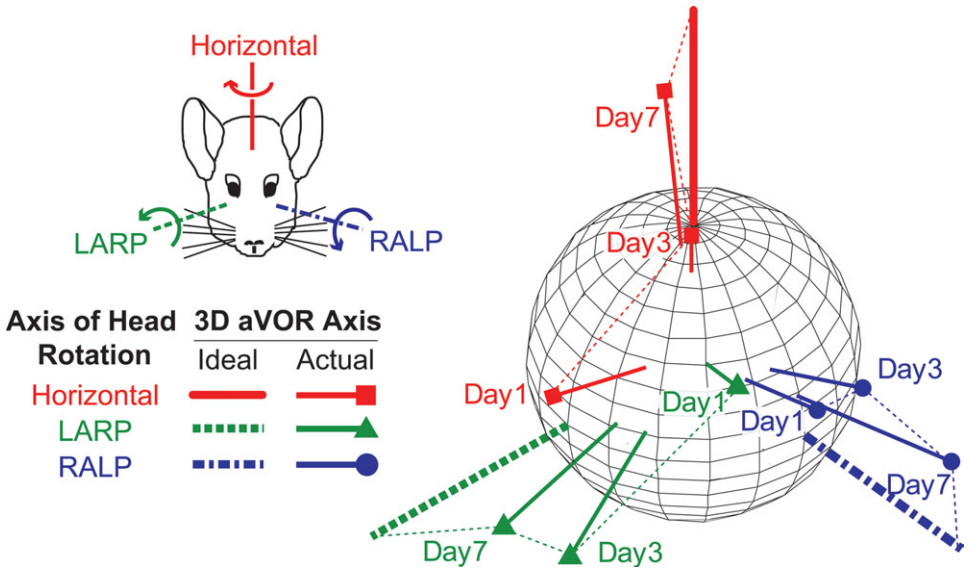

Fig. 5. Changes in axis of eye response for one chinchilla over 7 days of stimulation during continual MVP use. Each data vector shows the 3D axis and magnitude of VOR responses during whole-body 2 Hz, 50°/sec peak head rotations in darkness about the mean horizontal, LARP, and RALP SCC axes. Vector length indicates the peak response velocity; for comparison, thick axes depict inverse of 50°/sec peak head rotations about each canal axis. Progression over time toward the ideal response is apparent for each axis of head rotation, indicating that crossaxis adaptation corrects VOR misalignment over the first week of MVP use. Reprinted with permission from Dai et al., Exp Brain Res 2011, 210:595–606.

When only one labyrinth is functioning (e.g., after the opposite labyrinth is destroyed via surgery or unilateral intratympanic administration of an ototoxic drug), excitation–inhibition asymmetry is unmasked (Halmagyi et al., 2010). Immediately after unilateral injury, the imbalance in spontaneous input from the two labyrinths elicits a robust, sustained nystagmus with slow phases toward the injured side, as would be appropriate if the imbalance represented a head rotation toward the intact side rather than loss of input from the injured side. Vestibulo-cerebellar circuits eventually adapt to the new baseline over a few days to weeks via a process called *vestibular compensation*, adjusting synaptic strengths to account for the new status quo and ultimately recreating a relatively symmetric VOR for modest head movements (Sadeghi et al., 2010). However, asymmetry can still be unmasked by high-acceleration, high-velocity head rotations, for which excitatory head movements (moving the nose toward the intact side) can drive a primary afferent's firing rates up by >300% above the afferent's spontaneous discharge rate, whereas inhibitory head movements can only suppress firing rate by 100% (i.e., down to zero). During rapid rotations, VOR gain for head movement away from the normal labyrinth in a unilaterally vestibular-deficient human (Halmagyi et al., 1993; Della Santina et al., 2002), monkey, or chinchilla (Fridman et al., 2010) is typically <50% of the gain for head movement toward the normal labyrinth.

Like a single normal labyrinth, the MVP-implanted labyrinth in an otherwise BVD individual provides an inherently asymmetric input to central neurons mediating the VOR, because pulse frequency modulation of charge-balanced pulse stimuli delivered to the vestibular nerve is more effective at exciting the nerve (encoding head rotation *toward* the implanted labyrinth) than inhibiting it (encoding head rotation *away*). However, asymmetry is typically even greater for prosthetically evoked responses than for a single normal labyrinth. For example, in BVD chinchillas using an MVP set to baseline stimulus pulse rates approximating the mean normal afferent spontaneous rate, the electrically evoked VOR response to head rotation away from the implanted labyrinth can be as little as ~10% of the response to head rotation toward the implanted side (Della Santina et al., 2007; Davidovics et al., 2009; Davidovics et al., 2010; Fridman et al., 2010). This increase in asymmetry probably reflects the fact that downmodulation of MVP stimulus pulse rate to zero does not force primary afferent firing rates to zero. Although afferent spontaneous activity is only about 60% of normal after treatment with intratympanic gentamicin (Hirvonen et al., 2005), that residual afferent spontaneous activity creates a floor beneath which downmodulation of MVP input has little effect.

Bilateral implantation can solve this asymmetry problem (Gong et al., 2008); however, it is unlikely to be adopted readily into clinical practice before demonstration of success with unilaterally implanted MVPs, because it would incur substantially higher risk (e.g., of bilateral cochlear injury) and cost. Notably, although bilateral cochlear implantation has become common in the past decade, it only became widely accepted (and reimbursable by governmental and private insurance) after more than two decades of unilateral implantation demonstrated safety and efficacy (Wilson and Dorman, 2008).

Fortunately, it is possible to achieve a more symmetric VOR using a unilaterally implanted MVP that incorporates a baseline pulse rate well above the mean spontaneous discharge rate of vestibular primary afferents. The idea behind this method is to recalibrate central neurons to the artificially high baseline, which

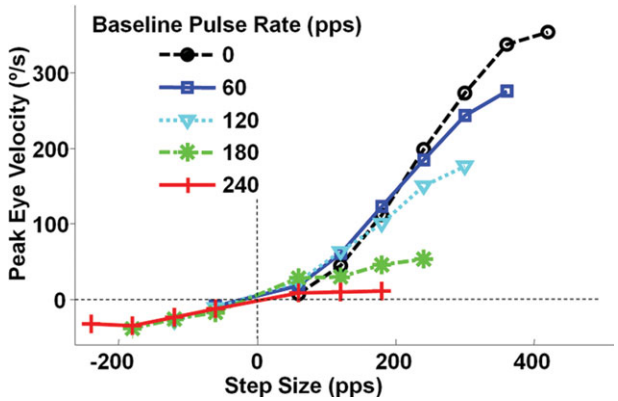

Fig. 6. Peak VOR eye velocity of a BVD chinchilla in response to steps in MVP pulse rate from baseline to maximum of 400 pulse/sec or minimum of 0 pulse/sec. Baseline stimulation pulse rate is indicated for each symbol. Responses become more symmetric as baseline rate is increased, but the increase in symmetry is owing more to loss of excitatory response than to the modest increases in inhibitory response. Reprinted with permission from Davidovics et al., ARO, 2009.

comes to represent the new normal when the head is stationary in a process analogous to vestibular compensation after unilateral labyrinthectomy. The increased baseline then allows a greater range over which downmodulation of prosthetic input can encode inhibitory head rotation. Experimental data show that when the baseline rate is set at about twice the mean primary afferent spontaneous rate, VOR responses are indeed more symmetric; however, the modest increase in inhibitory response comes at the expense of excitatory responses, which are reduced by up to an order of magnitude from the eye velocities observed when the baseline rate is set at or below the normal mean afferent discharge rate (Fig. 6) (Gong and Merfeld, 2002; Merfeld et al., 2007; Davidovics et al., 2009).

Efforts to further enhance prosthetic VOR symmetry without a reduction in VOR gain are on-going. Recently, Davidovics et al. showed that simultaneous modulation of both pulse frequency and pulse current amplitude (*comodulation*) allows one to achieve significantly greater inhibitory responses while still maintaining adequately large excitatory responses (Davidovics et al., 2011). For example, a step increase in pulse rate combined with a simultaneous step increase in pulse amplitude elicited VOR eye velocity 4× greater than the response to either stimulus parameter change alone, reaching responses as high as 2000°/sec (well above the ~500°/sec range needed to maintain stable gaze for most head movements of daily life). Inhibitory responses to simultaneous downmodulation of both pulse rate and amplitude were lower than the excitatory responses, but the absolute magnitude of inhibitory responses surpassed 300°/sec. Unfortunately, this increased inhibitory dynamic range comes at the price of increased misalignment, and hence efforts are now underway to combine the comodulation strategy with a variation of the "vector precompensation" correction strategy to achieve high-amplitude, symmetric, well-aligned responses.

An intriguing new approach to improving VOR asymmetry relies on a variation of a recently described vestibular rehabilitation technique. Working with unilaterally labyrinthectomized rhesus monkeys that had long since reached a steady state of vestibular compensation, Ushio et al. recently found that a training regimen in which a monkey is repeatedly subjected to passive, whole-body rotations toward the labyrinthectomized side while viewing a well-lit, high-contrast, stationary scene, VOR gain increases significantly for rotations toward that side without a reduction in VOR gain for contralesional head movements (Ushio et al., 2011). Applying the same approach to BVD rhesus monkeys using a unilateral MVP, Dai et al. achieved a similar improvement in inhibitory VOR gain without significant reduction in excitatory responses (Dai et al., 2012b).

Effects of Vestibular Electrode Array Implantation on Hearing

Cochlear implantation carries a modest risk of sensorineural vestibular injury (Migliaccio et al., 2005; Melvin et al., 2009), and hence it seems likely that implantation of electrodes in the labyrinth carries a risk to cochlear function. Fortunately, evidence from nonhuman primate studies suggests that vestibular implantation can be accomplished in humans without an unacceptable risk of hearing loss.

In chinchillas (which have a labyrinth about half the size of the human labyrinth), Tang et al. found that implantation of paired-wire electrodes in each of three SCCs caused hearing loss in four out of six implanted ears, whereas two ears maintained normal hearing (Tang et al., 2009). Although that study demonstrated the possibility of maintaining normal hearing, the rate of hearing loss it reported is hard to interpret in retrospect, because the use of air-conducted sound stimuli to measure auditory brainstem responses (ABRs) meant that observed hearing losses could have been due in whole or in part to mechanical/conductive effects related to immobilization of middle ear ossicles by the dental cement used to affix a head-holding post to each animal's cranium.

A subsequent study performed in rhesus monkeys resolved this question. Using electrode arrays similar to those designed for human implantation and employing a transmastoid surgical technique avoided interference with the ossicles and tympanic membrane, Dai et al. found that both ABR thresholds and distortion product otoacoustic emissions (DPOAE) in four monkeys before and after unilateral implantation of vestibular prosthesis electrodes in each of three left SCCs resulted in hearing being maintained to within 5–10 dB of normal at 1, 2, and 4 kHz (Dai et al., 2010b). Activation of the MVP caused ABR thresholds to increase by an additional ~5 dB and caused an insignificant fall in DPOAE amplitudes and DPOAE/noise floor ratios (Dai et al., 2010b). Animals exhibited no overt signs of perceiving an auditory sensation during MVP activation, and hence it is unclear whether the small changes noted in ABR and DPOAE after MVP activation represent spurious cochlear nerve activation or simply recording artifact due to the passage of MVP stimulus currents. Notably, cochlear implant users only rarely complain of vertigo with device use, so prosthetic stimulation of the cochlear nerve can be achieved without spurious stimulation of the vestibular nerve sufficient to elicit an abnormal

percept. Considering that multiple studies have demonstrated the ability to stimulate the anterior ampullary branch of the vestibular nerve while leaving the horizontal ampullary nerve branch relatively unaffected, it is likely that vestibular nerve stimulation can be achieved without generating tinnitus or otherwise interfering with hearing via current spread to the cochlear nerve.

Few data on hearing preservation after implantation of vestibular stimulating electrodes in humans are available, because the majority of the few studies so far reported have been performed in subjects undergoing cochlear implantation for bilateral deafness (Wall et al., 2007; Guyot et al., 2011a,b; van de Berg et al., 2011). Rubinstein et al. implanted one human subject with preexisting partial sensorineural hearing loss attributed to Meniere's disease using silicone and metal electrode arrays inserted into the thin limb of each SCC (Rubinstein et al., 2011). According to the authors, the subject suffered a severe sensorineural hearing loss in the implanted ear that later recovered partially (J. Rubinstein, personal communication).

Manipulations of the labyrinth comparable to those required for vestibular electrode implantation are routinely performed for plugging of SCC dehiscence or for gaining access to the skull base. Limb et al. reported that 19 out of 19 patients undergoing primary surgery for plugging or resurfacing of the superior SCC maintained hearing to within 5 dB of preoperative levels; however, 5 out of 5 patients undergoing revision surgery or plugging surgery after prior manipulation of the stapes did suffer a postoperative hearing loss (Limb et al., 2006). Interestingly, Kaylie et al. reported that removal of the entire thin segment of both the anterior and posterior SCCs and subsequent packing of wax into the stumps at the ampulla and common crus maintained hearing to within 10 dB of preoperative levels in 8 out of 8 patients undergoing a "transcrusal" approach to skull base tumors. In contrast to surgical plugging, this procedure necessarily disrupts the membranous labyrinth, and hence the fact that it can be performed without incurring significant cochlear injury bodes well for hearing outcomes in humans after implantation of vestibular electrode arrays.

A hybrid cochlear/vestibular implant has been proposed as a means for treating combined deafness and vestibular loss (Della Santina and Faltys, 2007). In individuals with useful preoperative hearing who are undergoing vestibular electrode implantation, the cochlear electrode of a hybrid device could potentially be banked in nearby temporalis musculature and left there as a safety net to be accessed and inserted into the cochlea during a second surgery if significant sensorineural hearing loss is noted after vestibular implantation.

Maintaining Continuous Prosthetic Stimulation

To encode inhibitory head rotations using biphasic charge-balanced pulses (which individually are almost always excitatory), a unilaterally implanted vestibular prosthesis must operate at a nonzero baseline rate representing zero head movement. As discussed above, this baseline rate is typically set above the mean spontaneous firing of vestibular afferents to leave adequate room for downmodulation. Once central vestibulo-cerebellar circuits have adapted to this baseline level of input, "spontaneous" nystagmus no longer occurs with the head at rest, and transient downmodulation of stimulus intensity below the baseline rate can effectively encode inhibitory movement.

Although the vestibular nervous system's ability to adapt to a new baseline provides a means to achieve bidirectional head motion encoding with a unilateral prosthesis, it also poses a technical challenge. Once an implant recipient has adapted to the new baseline, sudden cessation of stimulation owing to a loss of battery power can be perceived as a sudden inhibitory head rotation, causing vertigo, nystagmus, postural reflex movements, and other signs and symptoms of an acute unilateral imbalance of labyrinthine input.

Engineering approaches to addressing this challenge include incorporation of a rechargeable battery in the implantable portion of the stimulator, minimization of power consumption, use of power-saving safety modes, rigidly lockable percutaneous connectors for power and signal transmission between an external device and purely passive implanted electrode array, and other efforts to minimize the risk of decoupling between an implanted stimulator and an external power/signal transmission coil secured in place by magnetic attraction. Each of these approaches offers both advantages and disadvantages. Implanted batteries are preferable in many ways but require repeated surgeries for replacement during the lifetime of an implanted device. Percutaneous connectors offer a simple way to maximize power transmission efficiency while minimizing the risk of power loss due to battery drainage or disconnection, but they carry an increased risk of infection and are less preferable from a cosmetic point of view. Semi-implantable designs similar to existing cochlear implants can be made adequately secure through increases in the strength and/or number of retaining magnets, but no such arrangement can achieve an unbreakable link between internal and external devices.

Fortunately, adaptive neurophysiologic mechanisms can mitigate the risk, duration, and severity of vertigo caused by a break in power or signal transmission. Like ice skaters and astronauts who learn through repeated exposures to suppress vestibular reflexes that would otherwise cause a postrotatory nystagmus and postural instability immediately after completion of a sustained spin, one can learn to better tolerate sudden large transitions to a new baseline rate (including zero) through repeated exposures. Guinea pigs exposed to week-ON, week-OFF cycling of a single channel prosthesis exhibited a robust nystagmus lasting ~1,000 min when the device was first activated, as well as a prominent nystagmus in the opposite direction when the device was first deactivated a week later; however, the intensity and duration of post-transition nystagmus decreased with each power cycle, reaching ~20 s by the third ON→OFF transition (Fig. 7) (Merfeld et al., 2006). In contrast, the VOR response to sinusoidal modulation of prosthetic pulse rate remained stable despite this apparently learned response to ON→OFF and OFF→ON transitions, suggesting that the changes observed represent a form of *context-specific adaptation* in which a subject can learn to appropriately interpret and respond to a given change in primary afferent input as either a real head movement (for which nystagmus would be appropriate) or a spurious change in

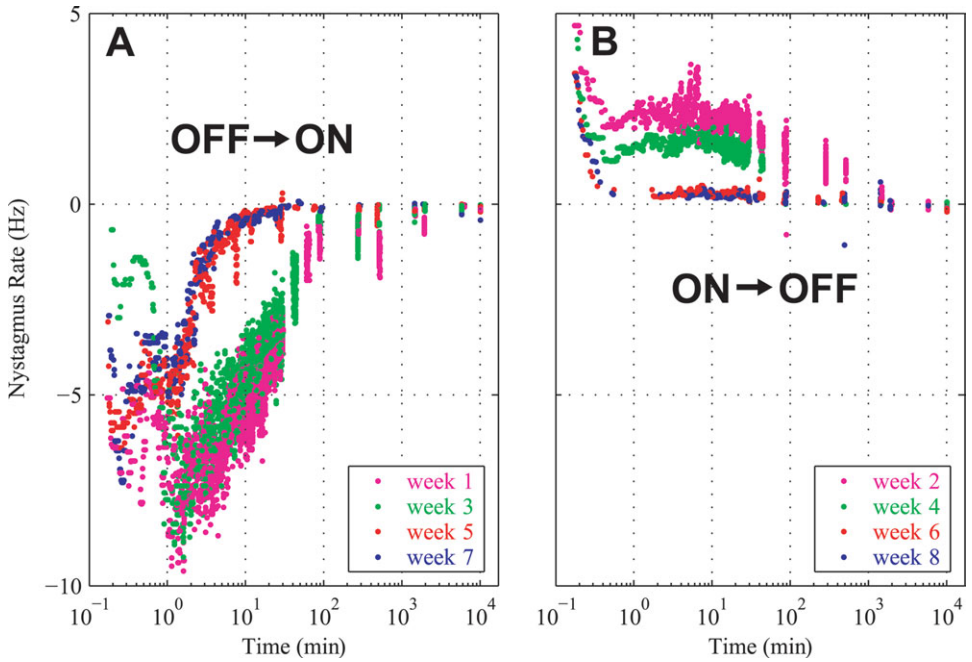

Fig. 7. Vestibulo-cerebellar circuits adapt to power cycling of the vestibular prosthesis delivering stimulation to a guinea pig horizontal branch of the vestibular nerve via implanted SCC electrode in 1-week-ON, 1-week-OFF experimental paradigm. When the prosthesis was first turned ON at the beginning of the first week (A, purple dots), the nystagmus lasted for ~1,000 min. When it was turned OFF at the beginning of the second week, nystagmus again lasted ~1,000 min (B, purple dots). Post-transition nystagmus duration decreased after each cycle. Nystagmus in response to turning the prosthesis ON at week 5 was ~10 min (blue dots), and nystagmus owing to turning the prosthesis OFF at week 6 lasted only ~20 sec (red dots). Reprinted with permission from Merfeld et al., IEEE Trans Biomed Eng, 2006, 53:2362–2372.

baseline rate (for which nystagmus should be suppressed).

Gyroscope Alignment

Whether gyroscopes are incorporated in the implanted processor or mounted outside the head using a percutaneous post or magnetic coupling, there will always be some variation in their relative orientation with respect to the SCCs they are meant to replace. As an MVP is designed to stimulate each SCC's ampullary nerve according to input from a gyroscope aligned with that SCC, misalignment between a gyroscope and the corresponding SCC is a potential source of misalignment between the actual head rotation and the VOR response elicited by an MVP.

Misalignment of sensors with SCCs can be overcome using a linear transformation analogous to the approach described above for correcting VOR misalignment owing to current spread (Merfeld, 2007). To maximize computational efficiency, the fitting matrix that corrects electrode stimulus intensities to account for current spread can be combined with a second matrix accounting for sensor orientation to form a single fitting matrix correcting for both sources of misalignment. The sensor/SCC mapping can be directly computed using data from computed tomography imaging of the implanted device and sensors with respect to the SCCs, but because the SCCs are mutually orthogonal and maintain a fairly consistent orientation with respect to palpable skull landmarks (Della Santina et al., 2005), an adequate approximation to the mapping matrix can be obtained by measuring sensor outputs during standardized head rotations about SCC axes approximated based on skull landmarks. Alternatively, devices that incorporate three-axis gyroscopes with integrated three-axis linear accelerometers (e.g., the Johns Hopkins MVP2) can report their orientation with respect to Earth-vertical when the head is kept momentarily motionless in other three orthogonal positions, and the resulting accelerometer signals can provide the elements of the sensor/SCC alignment matrix.

Otoconial Endorgans, Posture, and Gait

All vestibular prosthesis prototypes described in the literature so far have been designed to emulate SCC function while essentially ignoring the loss of utricular and saccular sensation. This situation stems from two facts.

First, restoring ampullary nerve activity to something approximating normal is much easier than restoring normal utricular and saccular nerve activity, because every axon in a given ampullary nerve encodes head rotation about the same 3D axis with the same polarity. In contrast, the utricular and saccular branches of the vestibular nerve each incorporate afferents that encode linear accelerations along a wide range of directions, with axons of different directional sensitivity being so closely adjacent that electrical current passed via an electrode inserted near either endorgan's sensory neuroepithelium is unlikely ever to achieve sufficient spatial selectivity to recreate a normal pattern of activity.

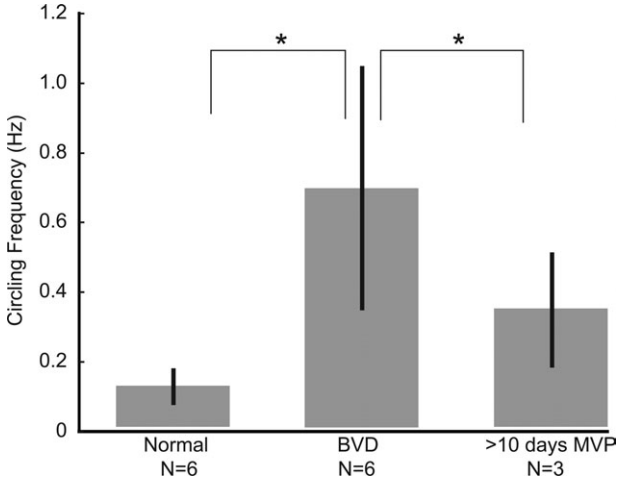

Fig. 8. MVP stimulation helps reduce abnormal circling ambulation behavior in BVD chinchillas. Unlike normal animals, chinchillas rendered BVD via bilateral intratympanic gentamicin injection tend to run in tight circles repeatedly when startled. After these BVD animals wear a head-mounted MVP for 10 days, the circling behavior diminishes significantly. (It apparently also remains greater than normal; however, that difference did not achieve statistical significance, possibly owing to the small sample size.) The circling behavior returns after MVP removal. Asterisks denote significance at $P < 0.05$. Reprinted with permission from Sun et al, Proceedings of the IEEE 33rd Annual EMBC Conference, 2011.

Second, utriculo- and sacculo-ocular reflexes (i.e., the *translational* VOR) and otoconial endorgan contributions to vestibulo-spinal reflexes that stabilize posture and gait are arguably less necessary than the *angular* VOR mediated by SCCs. The translational VOR's contribution to gaze stabilization is relatively small except when one is viewing objects close to one's eyes. Normal vestibular contributions to posture and gait are helpful, but their contributions can be more readily supplanted by proprioception, prediction, vision, and other systems than can be the angular VOR, which essentially acts alone for quick head movements during far-target viewing, such as those encountered when driving a car.

Despite a decision not to pursue restoration of otoconial end organ function until after SCC prostheses are more well-established, we have observed improvement in posture and gait among BVD animals using an MVP that conveys only angular motion information. Recently, Sun et al. quantified ambulatory behavior of chinchillas that were either normal, BVD after bilateral intratympanic gentamicin treatment, or BVD and treated with a head-mounted MVP encoding only head rotation and stimulating only via SCC electrodes (Sun et al., 2011). Although all BVD animals tended to run in tight circles, three animals circled significantly less when using the MVP than without it (Fig. 8), and animals also exhibited more exploratory behavior (a behavior typical of normal animals) when using the MVP. Circling frequency apparently remained greater than normal; however, that difference did not achieve statistical significance, possibly due to the small sample size. Failure to fully normalize circling frequency might be due to asymmetry of the prosthetically evoked vestibular percept, a lack of otolithic endorgan input, or other factors. Circling behavior returned when the prosthesis was turned off and when the MVP was set to a sham control condition in which it delivered constant baseline stimulation pulse rates that did not modulate with head movement.

Further elucidation of the effects of prosthetic SCC stimulation on posture and gait will benefit from transitioning these studies to nonhuman primates. Lewis et al. recently described the measurements of subjective horizontal and postural stability in rhesus monkeys trained to adjust a display to align with Earth-horizontal and to stand (on all four limbs) on a set of force plates (Lewis et al., 2012). Cohen et al. have developed a motion-capture system for assaying posture and gait in monkeys trained to run on a rotating platform, and they clearly demonstrated deficits in gait and step-placement precision after plugging of all SCCs (Cohen et al., 2009). Fitzpatrick, Day et al. have extensively characterized postural responses to transmastoid galvanic stimulation in human subjects (Fitzpatrick and Day, 2004), and variations on their experimental paradigms will likely be incorporated into assessments of human subjects using MVPs once clinical trials of such devices begin.

Minimizing Power Consumption

As maintaining continuous prosthetic stimulation is desirable both for convenience and to minimize the risk of vertigo due to an unexpected ON→OFF transition, minimizing power consumption to the point at which small batteries can drive a device for more than 24 hr per charging cycle is an important goal.

In contrast to cochlear implants (which typically consume only a few milliwatts), MVP power consumption is relatively high and is dominated by the power drawn by gyroscope sensors. Fortunately, sensor manufacturers have continually reduced their devices' power consumption in an effort to address the needs of high-volume consumer devices such as smart phones. Owing mainly to this effect, total power consumption fell from ~140 mW for the MVP1 (the first-generation Johns Hopkins MVP) to ~45 mW for the second-generation MVP2 (Della Santina et al., 2007; Chiang et al., 2011). The most recently announced, commercially available inertial sensor incorporates a three-axis gyroscope and three-axis accelerometer in one integrated circuit package that consumes <10 mW (MPU6000, InvenSense, Sunnyvale, CA). Even lower power consumption may ultimately be achieved using angular rotation sensors comprising fluid-filled tubes that mimic a SCC and micromachined pressure sensor diaphragms that mimic the operation of the cupula (Challa and Bhatti, 2010).

Other hardware components will become more important to the overall power budget as the efficiency of the commercially available gyroscopes improves. Converting prosthesis algorithms from software into application-specific integrated circuitry has been pursued as a way of improving the speed, size, and power efficiency of the overall device (Shkel and Zeng, 2006; Constandinou et al., 2008a,b; Constandinou et al., 2009).

Alternate Technologies for Prosthetic Stimulation of the Labyrinth via Implanted Electrodes

Transcutaneous/transmastoid galvanic stimulation (TGS) via large area electrodes stuck to the skin over

each postauricular region can elicit a modest but readily perceptible sensation of head movement (Fitzpatrick and Day, 2004). Typically, the ear nearest the TGS electrode delivering cathodic current is excited enough to elicit a modest (~5–10°/sec maximum slow phase) horizontal and torsional nystagmus and static ocular counter-roll consistent with nonspecific excitation of all five vestibular endorgans. However, neither the spatial selectivity nor the effective stimulus intensity of this approach is sufficient to recreate a useful 3D VOR for head rotations other than a slow rotation about a fixed anteroinferior rotation axis.

Infrared (IR) laser stimulation has recently garnered interest as a potential means to stimulate the cochlear nerve with spatial selectivity much greater than that achieved using electrical stimulation via electrodes implanted within the scala tympani (Richter et al., 2011). Rajguru et al. (2011) extended the approach to the vestibular labyrinth in toadfish, and Ahn et al. (2012) recently extended the same approach to the mammalian labyrinth. Contrary to the results obtained in mammalian cochlea and in other peripheral nerves (Wells et al., 2007), IR laser stimulation applied vestibular afferent neuron axons and somata yields little to no response in either toadfish or chinchillas in experiments published so far; however, IR directed at the crista (and presumably acting at vestibular hair cells) elicits a variety of changes in afferent firing rates, including excitatory, inhibitory, and mixed responses. Responses observed using single-unit recording techniques clearly demonstrate phase-locking to individual laser pulses, and hence this effect cannot be owing solely to the bulk movement of labyrinthine fluids that occurs during clinical caloric nystagmography testing.

Whether IR laser stimulation will prove useful as a therapeutic means of prosthetic stimulation is as yet unclear. VOR responses have not yet been demonstrated in response to IR stimuli, and despite the large changes of firing rate observed in individual vestibular afferents, the fact that IR can evoke an uncontrollable combination of excitatory, inhibitory, and mixed responses within different afferents within a given ampullary nerve will at least complicate the use of IR to encode head rotation. Nonetheless, IR laser stimulation may as yet have a therapeutic role, particularly if its high spatial resolution can be leveraged to achieve selective stimulation of many small patches in the utricle and saccule. Optical stimulation (whether IR or other spectral ranges) may also serve as an adjunct in combination with electrical stimulation or through incorporation of photosensitive channels via optogenetic techniques (Wang et al., 2012).

Seeking another alternative to electrical stimulation, Merfeld et al. described in concept a mechanical vestibular stimulator intended to amplify cupular movement via a piston or balloon implanted within a SCC. Although analogous mechanisms have long been used to great effect in bench research preparations to provide a "natural" stimulus to a SCC without having to rotate an animal (Rabbitt et al., 1995), the potential for clinical application of an implanted mechanical vestibular stimulator is unclear. Considering that most individuals with less-than-profound loss of vestibular sensation compensate adequately through reliance on other senses, the need for an implantable mechanical vestibular stimulator is less clear than the need for an electrical device that can address profound sensory loss. Such devices may therefore face the same sort of economic and medical decision-making constraints that have left little room for middle ear implantable hearing aids between conventional hearing aids and cochlear implants.

Various sensory substitution techniques have been advocated for conveying information about head motion to the central nervous system, including auditory stimuli delivered via headphones (Dozza et al., 2005; Hegeman et al., 2005), cutaneous sensation delivered by trunk vibrators (Wall, 2010), and electrotactile stimulation of the tongue (Tyler et al., 2003). Although each of these approaches has the potential to provide limited information about postural sway and head movement, none presents information to the central nervous system with sufficient resolution, specificity or speed to recreate a normal 3D VOR.

Clinical Feasibility Studies

Prosthetic electrical stimulation of the human labyrinth has only been reported for a small number of studies so far, and each involved a small number of subjects. None of these studies employed the 3D oculographic techniques necessary to measure 3D VOR misalignment, and hence the data they provide cannot fully characterize the extent of current spread between an electrode and nontarget nerve branches. Nonetheless, human studies have provided valuable data, and those general corroborate more extensive data sets from animal studies.

Wall et al. (2007) examined 2D eye movements in three individuals subjected to electrical stimulation of the singular nerve (i.e., the posterior SCC ampullary nerve) during cochlear implantation under local anesthesia. Using an approach similar to that developed for singular neurectomy, bone overlying the singular nerve was removed down to a ~100 μm layer, a monopolar electrode was positioned near the nerve, and biphasic pulse trains (200 μs/phase, 200 pulse/sec) were delivered for 10–60 sec while eye movements were recorded using 2D video-oculography. During these measurements, "spontaneous" nystagmus was present even without stimulation (suggesting irritation, injury, or thermal effects on nerve activity), but stimulus-evoked changes in slow phase nystagmus also occurred, and they were in the direction appropriate to excitation of the stimulated labyrinth. Varying pulse amplitude from 400 μA to 1 mA/phase changed nystagmus velocity from 30 to 50°/sec. Varying pulse frequency of a 500 μA, 200 μs/phase pulse train from 25 to 400 Hz evoked nystagmus that ranged from 0 to 40°/sec.

A follow-up study was conducted with three patients undergoing a labyrinthectomy for the treatment of Meniere's disease (Guyot et al., 2011a). In these experiments, an electrode was implanted in several positions in attempts to target the horizontal and the superior ampullary nerves. Responses were observed intraoperatively using 2D oculography. In all three individuals tested, eye movements were primarily horizontal with a smaller vertical component. Torsional responses could not be measured, and hence relative activation of the three SCCs could not be inferred with certainty. (Simultaneous excitation of all three left SCCs elicits a nystagmus that is horizontal on 2D oculography but

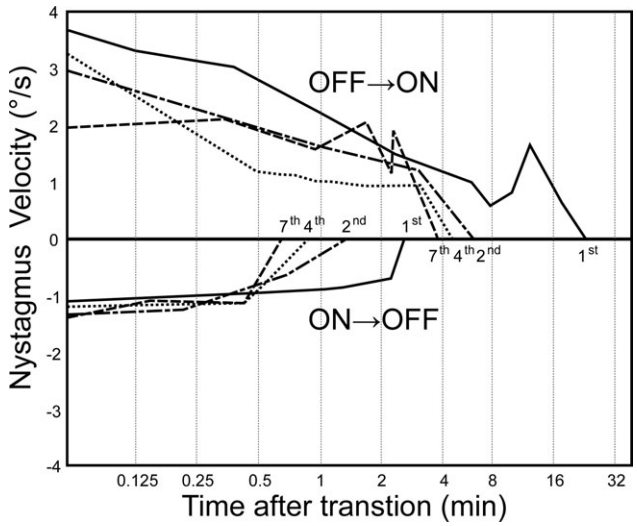

Fig. 9. A human subject implanted with a modified cochlear implant electrode in the vestibular labyrinth exhibited nystagmus lasting 27 min after initial device activation and ~3 min after initial deactivation. After several ON→OFF→ON cycles, devices reactivation elicited <4 min of nystagmus and deactivation elicited <1 min of nystagmus. Reproduced and printed with permission from Guyot et al., Ann Otol Rhinol Laryngol, 2011, 120:81–87.

includes a clockwise torsional component on 3D oculography; the torsional component results from vector superposition of the up/clockwise and down/clockwise responses driven by excitation of the left anterior and left posterior SCCs, respectively.) Two of the three subjects reported perception of rotation in the direction opposite the observed slow phase nystagmus. Facial movements indicating current spread to the facial nerve were observed for high-stimulation amplitudes at electrode positions, but it was possible to evoke 7–20°/sec nystagmus without facial activation.

Avoiding potential confounds owing to acute intraoperative nerve irritation requires examination of electrically evoked VOR responses in alert subjects who have had time to fully recover after permanent implantation. This has now been reported in two recent studies. During an otherwise standard cochlear implant surgery (in which 11 of the usual 12 electrodes on the implanted device were inserted per routine into the cochlea), Guyot et al. (2011b) implanted a monopolar electrode in the left posterior SCC. Stimulating with 200 pulse/sec biphasic pulse trains via this active electrode and a distant return, they observed a brisk nystagmus consistent with partially selective excitation of the implanted labyrinth's posterior SCC nerve and lasting ~27 min after initial activation (Fig. 9). As had previously been observed in guinea pigs, the duration of post-transition nystagmus decreased rapidly with and increasing number of ON/OFF cycles, reaching 3 min by the seventh OFF->ON change. Similarly, turning stimulation off resulted in 2 min of nystagmus after the first offset but only ~40 sec after the seventh offset.

These results suggest that (1) initial prosthesis activation can be accomplished with an acceptable duration of postactivation vertigo; (2) repeated ON→OFF→ON cycling may help subjects learn to gate in a form of context-specific VOR adaptation that allows them to rapidly adjust to new baseline rates; and (3) once trained, an implant user should be able to tolerate a sudden loss of power (e.g., due to battery discharge or disconnection of a head-mounted processor) without suffering a vertigo episode lasting more than a few minutes. Given that most candidates for vestibular implantation will have suffered significantly longer and more intense episodes of vertigo as part of the disease course that led to their acquired profound loss of vestibular sensation, comparatively brief bouts of vertigo after device activation or transient power loss should be tolerable.

In a recent study so far reported only in oral and abstract form, Rubinstein, Phillips et al. performed a similar chronic implantation in the ear of a single subject with unilateral Ménière's disease, using a modified cochlear implant intended not for continual sensory restoration but for transient activation to balance left and right vestibular tone during a Ménière's attack (Rubinstein et al., 2011). (This subject did not have profound loss of SCC function in either ear, and hence the goal was not to restore sensation but instead to modulate activity during an attack of spontaneous vertigo.) In this case, the modified cochlear implant had three linear electrode arrays, each containing a set of three electrodes intended for insertion into a given SCC. No electrodes were inserted into the cochlea. Unfortunately, the surgical intervention resulted in loss of residual hearing and natural SCC sensation in the implanted ear, but both of these ultimately recovered (personal communication, February 8, 2012). The patient's vertigo attacks ceased, limiting the opportunities to test the device's performance in its intended mode of action. However, electrically evoked nystagmus in approximately the desired direction was observed during acute stimulation sessions, and the implant user described vestibular percepts appropriate to the excitation of the targeted SCCs (Rubinstein et al., 2011). The stimulation threshold to evoke a VOR response was relatively high compared to animal studies (~300 μA), but sinusoidally modulating pulse amplitude to 60 μA above and below a 340 μA baseline at 3 Hz did elicit quasi-sinusoidal VOR responses. At this stimulation intensity, the evoked nystagmus had both horizontal and vertical components on 2D oculography.

DISCUSSION

Bilateral loss of vestibular sensation is disabling, more common than many conditions that have garnered much more attention from medical science, and associated with a significant increase in risk of falls. Although many individuals with severe loss of vestibular sensation ultimately do well following vestibular rehabilitation and cessation of vestibular suppressant medications, there is currently no effective clinical treatment for those who fail to compensate. These individuals—and the clinicians who treat them—are eager for an effective alternative that can partially or fully restore stable vision during head movement, ability to walk without fear of falling, and freedom from constant disequilibrium. Notably, "development of a vestibular prosthesis" was cited as among the "Top 10 Most Significant Projects in Otolaryngology Research for the Next 40 Years" in a recent survey of scientists at the National Institutes of

Health, ranking above "hair cell regeneration" (Zerhouni, 2007).

Fortunately, all technologies needed to make a MVP already exist, and market forces continue to drive improvements in the performance of individual elements such as inertial sensors. Coupled with extensive data from classic vestibular physiology literature, mounting evidence from more recent preclinical experiments in rodents and nonhuman primates supports the feasibility of a MVP for clinical use. Among other findings, these studies have shown:

1. A MVP can restore the 3D VOR sufficiently to significantly improve gaze stability.
2. A unilateral implant is adequate to drive both eyes and elicits a conjugate VOR; however, excitation–inhibition asymmetry is more pronounced for prosthetic stimulation than for a normal labyrinth in which hair cells can downmodulate neurotransmitter release sufficiently to drive an afferent's activity below the spontaneous rate.
3. Asymmetry of VOR responses driven by a unilateral implant can be significantly improved through adaptation to a supernormal baseline, comodulation of pulse frequency and current, rehabilitation paradigms that enhance responses to inhibitory head rotation, and bilateral implantation.
4. New electrode arrays incorporating silicone carriers that autoalign electrodes into positions identified as optimal using a computational model of the implanted labyrinth have simplified surgery and reliably yield good results. As model anatomy can be derived from CT and MRI scans, this approach can be applied to facilitate optimal design of electrode arrays for the human labyrinth.
5. Vestibular prosthesis implantation can be accomplished via an approach that is already familiar to ear surgeons, and implantation of a hybrid cochlear/vestibular electrode array can be performed to address loss of both balance and hearing in a single operative procedure.
6. Advances in stimulus protocol control software have rapidly boosted performance: in particular, vector precompensation (linear orthogonalization) significantly improves 3D VOR alignment, and comodulation of pulse frequency and current expands the dynamic range for excitatory and inhibitory head rotations.
7. Directional plasticity mechanisms within vestibulocerebellar circuits correct most residual VOR misalignment within 1 week of continuous prosthesis use.
8. Animals and humans exposed to ON/OFF cycling of constant rate stimulation develop an ability to tolerate those transitions, as indicated by a pronounced reduction in duration and intensity of post-transition nystagmus. This suggests a context-specific adaptation process through which patients can learn to tolerate device power interruptions caused by battery discharge or decoupling of an implant from its external system components.
9. Hearing is preserved to within ~10 dB in rhesus monkeys implanted with vestibular electrode arrays using an approach analogous to that used for humans.
10. Data in rodents suggest that restoration of head-motion-modulated activity on ampullary nerves improves postural and gait effects of vestibular deficiency, even when no attempt is made to restore normal utricular or saccular nerve activity.

Although only a small number of humans have been subjects in vestibular prosthetic stimulation experiments, initial experience in humans corroborates findings in animals, with the exception of a transient, incremental sensorineural hearing loss in the only individual implanted so far with multiple electrode arrays. However, data so far reported from these initial human studies must be considered with the caveat that responses to prosthetic vestibular stimulation in humans have not yet been quantified using the oculographic techniques required to fully characterize 3D VOR alignment.

Much remains to be done before an MVP system can enter routine clinical practice. Engineering priorities include further miniaturization of circuitry, optimization of stimulus paradigms, integration of system components for both stimulation and assessment of responses, reduction of power consumption, and eventual implementation of implantable rechargeable power storage technologies that would allow a prosthesis to run continuously without delivery of power and signals across the skin. Fortunately, vestibular prostheses are so similar to cochlear implants (and the motion sensors they require are so similar to those installed in consumer devices) that each of these priorities can be addressed using technology that already exists.

Although it is relatively straightforward to conceive a solution for every remaining technical challenge, regulatory and economic challenges pose a less predictable set of hurdles. Like cochlear implants, retinal implants, and all other neuroelectronic stimulators intended for lifelong implantation, vestibular prostheses are defined by the United States Food & Drug Administration as "significant risk" devices, a categorization that precludes expedited regulatory approval based on their substantial equivalence to cochlear implants that have already been approved for routine clinical use. Regulatory approval can therefore only be achieved through completion of clinical trials that are meticulously designed, rigorously administered, and adequately powered. Such trials are unavoidably expensive and time-consuming, and hence a collaborative approach drawing on contributions from academic labs, industrial partners, clinicians, patient groups, philanthropists, and government agencies supporting medical research will likely be required to make multichannel vestibular prostheses a reality for the chronically dizzy and disabled individuals who need them.

ACKNOWLEDGEMENT

The authors express their gratitude to Chenkai Dai, Americo A. Migliaccio, Natan S. Davidovics, Russell Hayden, Bryce Chiang, Mehdi Rahman, TjenSin Lie, Daniel Sun, Amit Patel, Thuy Melvin, Shan Tang, JoongHo Ahn, Lani Swarthout, Nicolas Valentin, Abderrahmane Hedjoudje, and other current and former members of the Johns Hopkins Vestibular NeuroEngineering Laboratory (VNEL) whose published work forms the

basis of this review. The authors also thank Lloyd B. Minor, John P. Carey, Timothy E. Hullar, David Lasker, HongJu Park, Sophia Lyford-Pike, Michael Schubert, Iee-Ching Wu Anderson and other members of the Johns Hopkins Laboratory of Vestibular Neurophysiology, whose work formed the foundation upon which VNEL research was built. Dr. Della Santina is the CEO and an owner of Labyrinth Devices, LLC, a start-up company he founded to support commercialization of vestibular prosthesis technology. The terms of this arrangement are being managed by the Johns Hopkins University in accordance with its conflict of interest policies. All data from studies performed in the Johns Hopkins Vestibular NeuroEngineering Laboratory were obtained using protocols approved by the Johns Hopkins Animal Care and Use Committee.

LITERATURE CITED

Ahn JH, Lasker D, Dai C, Fridman GY, Della Santina CC. 2012. Infra-red laser stimulation modulates vestibular nerve afferent responses in the mammalian labyrinth. Midwinter Meeting of the Association for Research in Otolaryngology. 2–26-2012.

Berger SA, Goldsmith W, Lewis ER, editors. 1996. Introduction to bioengineering. New York: Oxford Universiy Press. p 339–360.

Bonham BH, Litvak LM. 2008. Current focusing and steering: modeling, physiology, and psychophysics. Hear Res 242:141–153.

Carey JP, Della Santina CC. 2005. Principles of applied vestibular physiology. In: Cummings CW, editor. Otolaryngology: Head & Neck Surgery. Philadelphia: Elsevier.

Carey JP, Minor LB, Peng GC, Della Santina CC, Cremer PD, Haslwanter T. 2002. Changes in the three-dimensional angular vestibulo-ocular reflex following intratympanic gentamicin for Meniere's disease. J Assoc Res Otolaryngol 3:430–443.

Challa P, Bhatti, PT. 2010. A Micromachine Cupula: Toward a Low-Power Biomimetic Angular Velocity Sensor for a Vestibular Prosthesis. Association for Research in Otolaryngology Midwinter Meeting. 2–6-2010.

Chiang B, Fridman GY, Dai C, Rahman MA, Della Santina C. 2011. Design and performance of a multichannel vestibular prosthesis that restores semicircular canal sensation in macaques. IEEE Trans Neural Syst Rehabil Eng IEEE-TNSRE-2010–0085.R2.

Cohen B, Suzuki, JI. 1963. Eye movements induced by ampullary nerve stimulation. Am J Physiol 204:347–351.

Cohen B, Suzuki J, Bender MB. 1964. Eye movements from semicircular canal nerve stimulation in cat. Ann Otol Rhinol Laryngol 73:153–169.

Cohen B, Xiang Y, Yakushin SB, Kunin M, Raphan T, Minor L, Della Santina CC. 2009. Effect of canal plugging on quadrupedal locomotion in monkey. Ann N Y Acad Sci 1164:89–96.

Collewijn H, Smeets JB. 2000. Early components of the human vestibulo-ocular response to head rotation: latency and gain. J Neurophysiol 84:376–389.

Constandinou TG, Georgiou J, Toumazou C. 2008a. A fully-integrated semicircular canal processor for an implantable vestibular prosthesis. 15th IEEE International Conference on Electronics, Circuits and Systems.

Constandinou T, Georgiou J, Toumazou C. 2008b. A partial-current-steering biphasic stimulation driver for vestibular prostheses. IEEE Trans Biomed Circuits Syst 2:106–113.

Constandinou TG, Georgiou J, Toumazou, C. 2009. A neural implant ASIC for the restoration of balance in individuals with vestibular dysfunction. IEEE International Symposium on Circuits and Systems (ISCAS).

Dai C, Ahn JH, Fridman GY, Rahman MA, Della Santina CC. 2012a. Electrically-evoked compound action potentials and 3D vestibulo-ocular reflex are correlated to each other and to electrode position in rhesus monkays using a multichannel vestibular prosthesis. Midwinter Meeting of the Association for Research in Otolaryngology. 2–2-2012.

Dai C, Fridman GY, Chiang B, Davidovics N, Della Santina CC. 2010a. 3D angular VOR adaptation to chronic motion-modulated multi-channel prosthetic stimulation of semicircular canal ampullary nerves. Midwinter Meeting of the Association for Research in Otolaryngology. 2–10-2010.

Dai C, Fridman GY, Chiang B, Davidovics NS, Melvin TA, Cullen KE, Della Santina CC. 2011a. Cross-axis adaptation improves 3D vestibulo-ocular reflex alignment during chronic stimulation via a head-mounted multichannel vestibular prosthesis. Exp Brain Res 210:595–606.

Dai C, Fridman GY, Davidovics NS, Chiang B, Ahn JH, Della Santina CC. 2011b. Restoration of 3D vestibular sensation in rhesus monkeys using a multichannel vestibular prosthesis. Hear Res 281:74–83.

Dai C, Fridman GY, Della Santina CC. 2010b. Effects of vestibular prosthesis electrode implantation and stimulation on hearing in rhesus monkeys. Hear Res 277:204–210.

Dai C, Lasker D, Ahn JH, Fridman GY, Rahman MA, Della Santina CC. 2012b. Repeated unidirectional rotations reduce vestibulooocular reflex gain asymmetry in rhesus monkeys using a unilateral multichannel vestibular prosthesis. Midwinter Meeting of the Association for Research in Otolaryngology. 2–26-2012.

Davidovics N, Fridman GY, Della Santina CC. 2009. Linearity of stimulus-response mapping during semicircular canal stimulation using a vestibular prosthesis. Association for Research in Otolaryngology. Baltimore.

Davidovics NS, Fridman GY, Chiang B, Della Santina CC. 2010. Effects of biphasic current pulse frequency, amplitude, duration and interphase gap on eye movement responses to prosthetic electrical stimulation of the vestibular nerve. IEEE Trans Neural Syst Rehabil Eng 2011;19:84–94.

Davidovics N, Fridman GY, Della Santina CC. Co-modulation of stimulus rate and current from elevated baselines expands head motion encoding range of the vestibular prosthesis. Exp Brain Res in press, DOI: 10.1007/s00221–012-3025–8.

Davidovics NS, Rahman MA, Dai C, Ahn JH, Fridman GY, Della Santina CC. 2012. Concurrent modulation of pulse frequency and current with coordinate transformation yields improved 3D VOR dynamic range, symmetry and alignment in monkeys using a multichannel vestibular prosthesis. ARO Midwinter Meeting. 2–15-2012.

Della Santina CC, Cremer PD, Carey JP, Minor LB. 2002. Comparison of head thrust test with head autorotation test reveals that the vestibulo-ocular reflex is enhanced during voluntary head movements. Arch Otolaryngol Head Neck Surg 128:1044–1054.

Della Santina CC, Faltys MA. 2007. Dual cochlear/vestibular stimulator with control signals derived from motion and speech signals. US Pat 7,225,028. 5–29-2007.

Della Santina CC, Hoffman H. 2010. Prevalence and impact of bilateral vestibular deficiency (BVD): results from the 2008 United States National Health Interview Servey. J Vestib Res 20: 243–244.

Della Santina CC, Migliaccio AA, Patel AH. 2007. A multichannel semicircular canal neural prosthesis using electrical stimulation to restore 3-D vestibular sensation. IEEE Trans Biomed Eng 54: 1016–1030.

Della Santina CC, Potyagaylo V, Migliaccio AA, Minor LB, Carey JP. 2005. Orientation of human semicircular canals measured by three-dimensional multiplanar CT reconstruction. J Assoc Res Otolaryngol 6:191–206.

Dozza M, Chiari L, Horak FB. 2005. Audio-biofeedback improves balance in patients with bilateral vestibular loss. Arch Phys Med Rehabil 86:1401–1403.

Ewald JR. 1892. Physiologische Untersuchungen uber das Endorgan des Nervus Octavus. Wiesbaden, Germany: Bergmann.

Fitzpatrick RC, Day BL. 2004. Probing the human vestibular system with galvanic stimulation. J Appl Physiol 96:2301–2316.

Fridman GY, Davidovics NS, Dai C, Migliaccio AA, Della Santina CC. 2010. Vestibulo-ocular reflex responses to a multichannel vestibular prosthesis incorporating a 3D coordinate transformation for correction of misalignment. J Assoc Res Otolaryngol 11: 367–381.

Gillespie MB, Minor LB. 1999. Prognosis in bilateral vestibular hypofunction. Laryngoscope 109:35–41.
Gong WS, Haburcakova C, Merfeld DM. 2008. Vestibulo-ocular responses evoked via bilateral electrical stimulation of the lateral semicircular canals. IEEE Trans Biomed Eng 55:2608–2619.
Gong WS, Merfeld DM. 2000. Prototype neural semicircular canal prosthesis using patterned electrical stimulation. Ann Biomed Eng 28:572–581.
Gong WS, Merfeld DM. 2002. System design and performance of a unilateral horizontal semicircular canal prosthesis. IEEE Trans Biomed Eng 49:175–181.
Grossman GE, Leigh RJ, Abel LA, Lanska DJ, Thurston SE. 1988. Frequency and velocity of rotational head perturbations during locomotion. Exp Brain Res 70:470–476.
Grossman GE, Leigh RJ, Bruce EN, Huebner WP, Lanska DJ. 1989. Performance of the human vestibloocular reflex during locomotion. J Neurophysiol 62:264–271.
Grunbauer WM, Dieterich M, Brandt T. 1998. Bilateral vestibular failure impairs visual motion perception even with the head still. Neuroreport 9:1807–1810.
Guyot JP, Sigrist A, Pelizzone M, Feigl GC, Kos MI. 2011a. Eye movements in response to electrical stimulation of the lateral and superior ampullary nerves. Ann Otol Rhinol Laryngol 120:81–87.
Guyot JP, Sigrist A, Pelizzone M, Kos MI. 2011b. Adaptation to steady-state electrical stimulation of the vestibular system in humans. Ann Otol Rhinol Laryngol 120:143–149.
Halmagyi GM, Curthoys IS, Dai MJ. 1993. The human vestibulo-ocular reflex after unilateral vestibular deafferentation: the results of high-acceleration impulsive testing. In: Sharpe JA, Barber HO, editors. The vestibulo-ocular reflex and vertigo. New York: Raven Press. p 45–54.
Halmagyi GM, Weber KP, Curthoys IS. 2010. Vestibular function after acute vestibular neuritis. Restor Neurol Neurosci 28:37–46.
Hayden R, Sawyer S, Frey E, Mori S, Migliaccio AA, Della Santina CC. 2011. Virtual labyrinth model of vestibular afferent excitation via implanted electrodes: validation and application to design of a multichannel vestibular prosthesis. Exp Brain Res 210:623–640.
Hedjoudje A, Hayden R, Dai C, Ahn JH, Rahman MA, Ben Johny M, Olds K, Mori S, Della Santina CC. 2012. Virtual labyrinth model accurately predicts responses to stimulation using a multichannel vestibular prosthesis in rhesus monkeys. Midwinter Meeting of the Association for Research in Otolaryngology. 2–26-2012.
Hegeman J, Honegger F, Kupper M, Allum JHJ. 2005. The balance control of bilateral peripheral vestibular loss subjects and its improvement with auditory prosthetic feedback. J Vestib Res 15:109–117.
Herdman SJ. 1998. Role of vestibular adaptation in vestibular rehabilitation. Otalaryngol Head Neck Surg 119:49–54.
Herdman SJ, Blatt PJ, Schubert MC. 2000. Vestibular rehabilitation of patients with vestibular hypofunction or with benign paroxysmal positional vertigo. Curr Opin Neurol 13:39–43.
Hirvonen TP, Minor LB, Hullar TE, Carey JP. 2005. Effects of intratympanic gentamicin on vestibular afferents and hair cells in the chinchilla. J Neurophysiol 93:643–655.
Leigh RJ, Zee DS. 1999. The neurology of eye movement. 3rd ed. New York: Oxford University Press.
Lewis R, Haburcakova C, Gong W, Lee D, Merfeld DM. 2012. Vestibular contributions to tilt perception in nonhuman primates. Midwinter Meeting of the Association for Research in Otolaryngology. 2–26-2012.
Lewis RF, Gong WS, Ramsey M, Minor L, Boyle R, Merfeld DM. 2002. Vestibular adaptation studied with a prosthetic semicircular canal. J Vestib Res 12:87–94.
Lewis RF, Merfeld DM and Gong WS. 2001. Cross-axis vestibular adaptation produced by patterned electrical stimulation. Neurology 56:A18.
Limb CJ, Carey JP, Srireddy S, Minor LB. 2006. Auditory function in patients with surgically treated superior semicircular canal dehiscence. Otol Neurotol 27:969–980.
Lowenstein OE, Sand A. 1940. The mechanism of the semi-circular canals: a study of responses of single fiber preparatons to angular accelerations and to rotation at constant speed. Proc R Soc London B Biol Sci 129:256–275.
Macherey O, Deeks JM, Carlyon RP. 2011. Extending the limits of place and temporal pitch perception in cochlear implant users. J Assoc Res Otolaryngol 12:233–251.
Melvin TA, Della Santina CC, Carey JP, Migliaccio AA. 2009. The effects of cochlear implantation on vestibular function. Otol Neurotol 30:87–94.
Merfeld DM. 2007. Sensor signal alignment. US Patent and Trademark Office (20070055331). USA.
Merfeld DM, Gong WS, Morrissey J, Saginaw M, Haburcakova C, Lewis RF. 2006. Acclimation to chronic constant-rate peripheral stimulation provided by a vestibular prosthesis. IEEE Trans Biomed Eng 53:2362–2372.
Merfeld DM, Haburcakova C, Gong W, Lewis RF. 2007. Chronic vestibulo-ocular reflexes evoked by a vestibular prosthesis. IEEE Trans Biomed Eng 54:1005–1015.
Merrill DR, Bikson M, Jefferys JGR. 2005. Electrical stimulation of excitable tissue: design of efficacious and safe protocols. J Neurosci Methods 141:171–198.
Migliaccio AA, Della Santina CC, Carey JP, Niparko JK, Minor LB. 2005. The vestibulo-ocular reflex response to head impulses rarely decreases after cochlear implantation. Otol Neurotol 26:655–660.
Minor LB. 1998. Gentamicin-induced bilateral vestibular hypofunction. J Am Med Assoc 279:541–544.
National Center for Health Statistics. National Health Interview Survey 2008. 2008. National Institute on Deafness and Other Communication Disorders and United States Public Health Service.
Nie K, Bierer SM, Ling L, Oxford T, Rubinstein JT, Phillips JO. 2011. Characterization of the electrically evoked compound action potential of the vestibular nerve. Otol Neurotol 32:88–97.
Rabbitt RD, Boyle R, Highstein SM. 1995. Mechanical indentation of the vestibular labyrinth and its relationship to head rotation in the toadfish, Opsanus tau. J Neurophysiol 73:2237–2260.
Rahman MA. 2011. System Integration of a Multichannel Vestibular Prosthesis. Dissertation.
Rajguru SM, Richter CP, Matic AI, Holstein GR, Highstein SM, Dittami GM, Rabbitt RD. 2011. Infrared photostimulation of the crista ampullaris. J Physiol 589:1283–1294.
Richter CP, Rajguru SM, Matic AI, Moreno EL, Fishman AJ, Robinson AM, Suh E, Walsh JT. 2011. Spread of cochlear excitation during stimulation with pulsed infrared radiation: inferior colliculus measurements. J Neural Eng 8:056006.
Robblee LS, Rose TL. 1990. Electrochemical guidelines for selection of protocols and electrode materials for neural stimulation, in Neural Prostheses: Fundamental Studies (Agnew WF and McCreery DB, eds.). Prentice Hall. Englewood Cliffs, NJ. pp. 25–66.
Rose TL, Robblee LS. 1990. Electrical-stimulation with Pt electrodes. 8. Electrochemically safe charge injection limits with 0.2 ms pulses. IEEE Trans Biomed Eng 37:1118–1120.
Rubinstein JT, Phillips J, Nai K, Ling L, Bierer S, Jameson E, Oxford T. 2011. Clinical, scientific, and regulatory roadmap for a human vestibular implant. ARO Midwinter Meeting. 2–1-2011.
Sadeghi SG, Minor LB, Cullen KE. 2006. Dynamics of the horizontal vestibuloocular reflex after unilateral labyrinthectomy: response to high frequency, high acceleration, and high velocity rotations. Exp Brain Res 175:471–484.
Sadeghi SG, Minor LB, Cullen KE. 2010. Neural correlates of motor learning in the vestibulo-ocular reflex: dynamic regulation of multimodal integration in the macaque vestibular system. J Neurosci 30:10158–10168.
Schultheis LW, Robinson DA. 1981. Directional plasticity of the vestibulo-ocular reflex in the cat. Ann NY Acad Sci 374:504–512.
Shannon RV. 1992. A model of safe levels for electrical-stimulation. IEEE Trans Biomed Eng 39:424–426.
Shepherd RK. 1986. Cochlear Prosthesis: Safety Investigations, Dissertation, University of Melbourne.
Shepherd RK, Javel E. 1999. Electrical stimulation of the auditory nerve: II. Effect of stimulus waveshape on single fibre response properties. Hear Res 130:171–188.
Shepherd RK, Matsushima J, Millard RE, Clark GM. 1991. Cochlear pathology following chronic electrical stimulation using non charge balanced stimuli. Acta Otolaryngol 111:848–860.

Shkel AM, Zeng FG. 2006. An electronic prosthesis mimicking the dynamic vestibular function. Audiol and Neuro-Otology 11:113–122.

Sun DQ, Rahman MA, Fridman GY, Chiang B, Dai C, Della Santina CC. 2011. Chronic stimulation of the semicircular canals using a multichannel prosthesis: effects on locomotion and angular vestibulo-ocular reflex in chinchillas. Proceedings of the IEEE 33rd Annual EMBC Conference. 9–10-2011.

Suzuki JI, Cohen B. 1964. Head eye body + limb movements from semicircular canal nerves. Exp Neurol 10:393–405.

Suzuki JI, Goto K, Tokumasu K, Cohen B. 1969. Implantation of electrodes near individual vestibular nerve branches in mammals. Ann Otol Rhinol Laryngol 78:815–826.

Tabak S, Collewijn H, Boumans LJ, Van der Steen J. 1997a. Gain and delay of human vestibulo-ocular reflexes to oscillation and steps of the head by a reactive torque helmet II.Vestibular-deficient subjects. Acta Oto-Laryngologica 117:796–809.

Tabak S, Collewijn H, Boumans LJJM, Van der Steen J. 1997b. Gain and delay of human vestibulo-ocular reflexes to oscillation and steps of the head by a reactive torque helmet. I. Normal subjects. Acta Otolaryngol 117:785–795.

Tang S, Melvin TAN, Della Santina CC. 2009. Effects of semicircular canal electrode implantation on hearing in chinchillas. Acta Otolaryngol 129:481–486.

Tullio P. 1929. Das Ohr und die Entstehung der Sprache und Schrift. Berlin: Urban & Schwarzenberg.

Tyler M, Danilov Y, Bach YR. 2003. Closing an open-loop control system: vestibular substitution through the tongue. J Integr Neurosci 2:159–164.

Ushio M, Minor LB, Della Santina CC, Lasker DM. 2011. Unidirectional rotations produce asymmetric changes in horizontal VOR gain before and after unilateral labyrinthectomy in macaques. Exp Brain Res 210:651–660.

van de Berg R, Guinand N, Stokroos RJ, Guyot JP, Kingma H. 2011. The vestibular implant: quo vadis? Front Neurol 2: 47.

Wall C, III. 2010. Application of vibrotactile feedback of body motion to improve rehabilitation in individuals with imbalance. J Neurol Phys Ther 34:98–104.

Wall C, Kos MI, Guyot JP. 2007. Eye movements in response to electric stimulation of the human posterior ampullary nerve. Ann Otol Rhinol Laryngol 116:369–374.

Wang J, Wagner F, Borton DA, Zhang J, Ozden I, Burwell RD, Nurmikko AV, van Wagenen R, Diester I, Deisseroth K. 2012. Integrated device for combined optical neuromodulation and electrical recording for chronic in vivo applications. J Neural Eng 9:016001.

Wells J, Konrad P, Kao C, Jansen ED, Mahadevan-Jansen A. 2007. Pulsed laser versus electrical energy for peripheral nerve stimulation. J Neurosci Methods 163:326–337.

Wilson BS, Dorman MF. 2008. Cochlear implants: a remarkable past and a brilliant future. Hear Res 242:3–21.

Yakushin SB, Tarasenko Y, Raphan T, Suzuki J, Della Santina CC, Minor LB, Cohen B. 2009. Modification of the cervico-ocular reflex by canal plugging. Ann N Y Acad Sci 1164:60–67.

Zerhouni, E. 2007. NIH Director's Address to American Academy of Otolaryngology-Head & Neck Surgery Annual Meeting.